

Cenozoic Age Counterclockwise Rotation in the Northwest End of the Sierras Pampeanas, Argentina

Adolfo Antonio Gutiérrez^{1*} , Ricardo Mon^{1,2}, Clara Eugenia Cisterna^{1,2}, Uwe Altenberger³, Ahmad Arnous^{1,2}

¹Faculty of Natural Sciences and IML, National University of Tucumán, San Miguel de Tucumán, Tucumán Province, Argentina

²National Council for Scientific and Technical Research, Buenos Aires, Argentina

³Institute for Earth and Environmental Sciences, Potsdam University, Potsdam-Golm, Germany

Email: *gutierrez.aa@hotmail.com

How to cite this paper: Gutiérrez, A.A., Mon, R., Cisterna, C.E., Altenberger, U. and Arnous, A. (2023) Cenozoic Age Counterclockwise Rotation in the Northwest End of the Sierras Pampeanas, Argentina. *Open Journal of Geology*, 13, 345-383.

<https://doi.org/10.4236/ojg.2023.135018>

Received: February 14, 2023

Accepted: May 27, 2023

Published: May 30, 2023

Copyright © 2023 by author(s) and Scientific Research Publishing Inc. This work is licensed under the Creative Commons Attribution International License (CC BY 4.0).

<http://creativecommons.org/licenses/by/4.0/>



Open Access

Abstract

Investigations into the Andean oroclinal revealed a counterclockwise rotation of about 37° in the north and a clockwise rotation of about 29° in the south. This rotation would have started in the Eocene because the Nazca and South American plates converged. The transition zone between the Puna and the Sierras Pampeanas has a clockwise rotation pattern. Our new data show that the NE convergence of the Nazca and South American plates caused the counterclockwise rotation around the NW end of the Sierras Pampeanas. The temperature rise during a magmatic activity at 13 Ma would have favored a counterclockwise rotation of the mountain blocks of about 20° on a detachment zone within 10 to 15 km of depth. These range rotations generated local stress tensors trending NE and NW, facilitating the development of valleys, basins, mineralized dikes, mineral deposits, and alluvial fans separated from their origin. The Atajo fault shows both ductile and brittle characteristics. A mylonitic belt from the Sierra de Aconquija was juxtaposed on the rocks of the Ovejería Block and the Farallón Negro Volcanic Complex by reverse vertical displacement, and a dextral horizontal component of displacement resulted in curvatures that gave rise to pull-apart basins and step over features. The Santa Maria Valley, Campo del Arenal, Hualfín Valley, and Pipanaco salt flat most likely constituted a vast early Miocene basin rarely interrupted by low feature relief.

Keywords

Neotectonic, Counterclockwise Rotation, Andes, Sierras Pampeanas, Transcurrent Faults, Morphotectonic

1. Introduction

The study area is at the northwest end of Argentina's Sierras Pampeanas, on the continental edge of the retro arc, on the 150 - 175 km depth lines of the Wadatti-Benioff zone [1], where the Farallón Negro Volcanic Complex gave rise to porphyry Cu-Au and epithermal Au deposits (Mn, Ag, As, Pb, Zn) (**Figure 1** and **Figure 2**). Given the depth of the Wadatti-Benioff zone, most seismic foci occur between 150 and 300 km deep, with others occurring less frequently between 70 and 150 km deep (**Figure 2**).

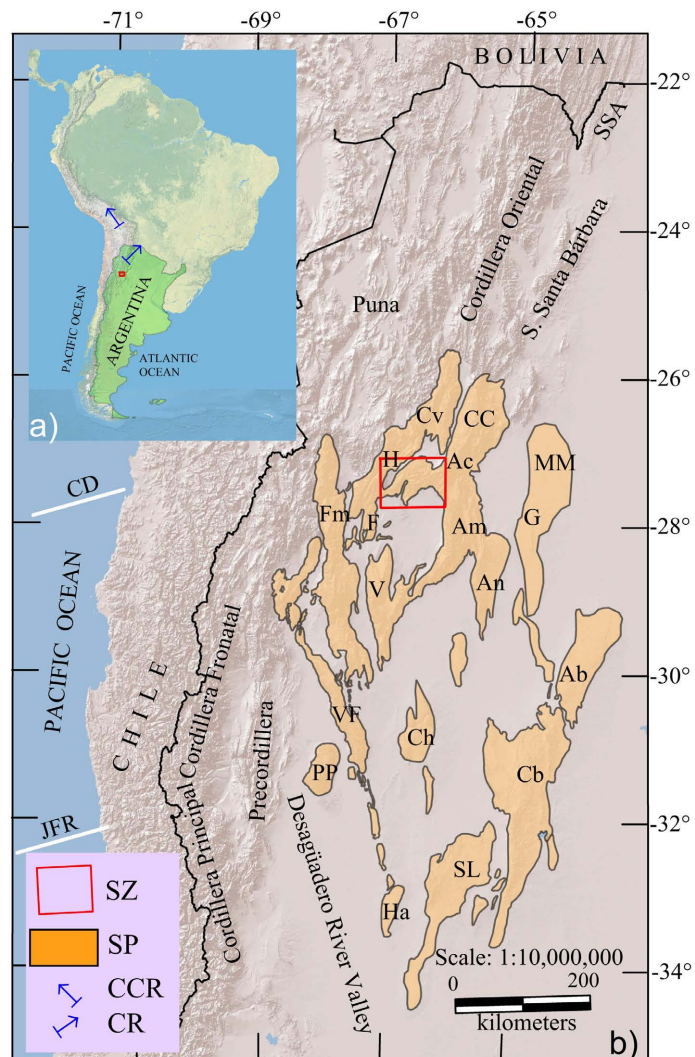


Figure 1. (a) Argentina's location in South America and an indication of paleomagnetic rotations. (b) Regional scheme of the Sierras Pampeanas, NW Argentina, and study area location. SZ: Study zone. SP: Sierras Pampeanas. CCR: Counterclockwise rotation. CR: Clockwise rotation. CD: Copiapó Ridge. JFR: Juan Fernández Ridge. The white lines indicate the trajectories of the ridges. SSA: Sierras Subandinas. Cv: Las Cuevas Range. CC: Cumbres Calchaquíes. H: Hualfín Range. Ac: Sierra de Aconquija. MM: Dorsal Mujer Muerta. Fm: Famatina. F: Fiambalá Range. Am: Ambato Block. G: Guasayán Range. V: Velazco Range. An: Ancasti Range. VF: Valle Fértil Range. Ch: Chepes Range. Ab: Ambargasta Range. PP: Pie de Palo Range. Cb: Sierras de Córdoba. Ha: La Huerta Range. SL: San Luís Range.

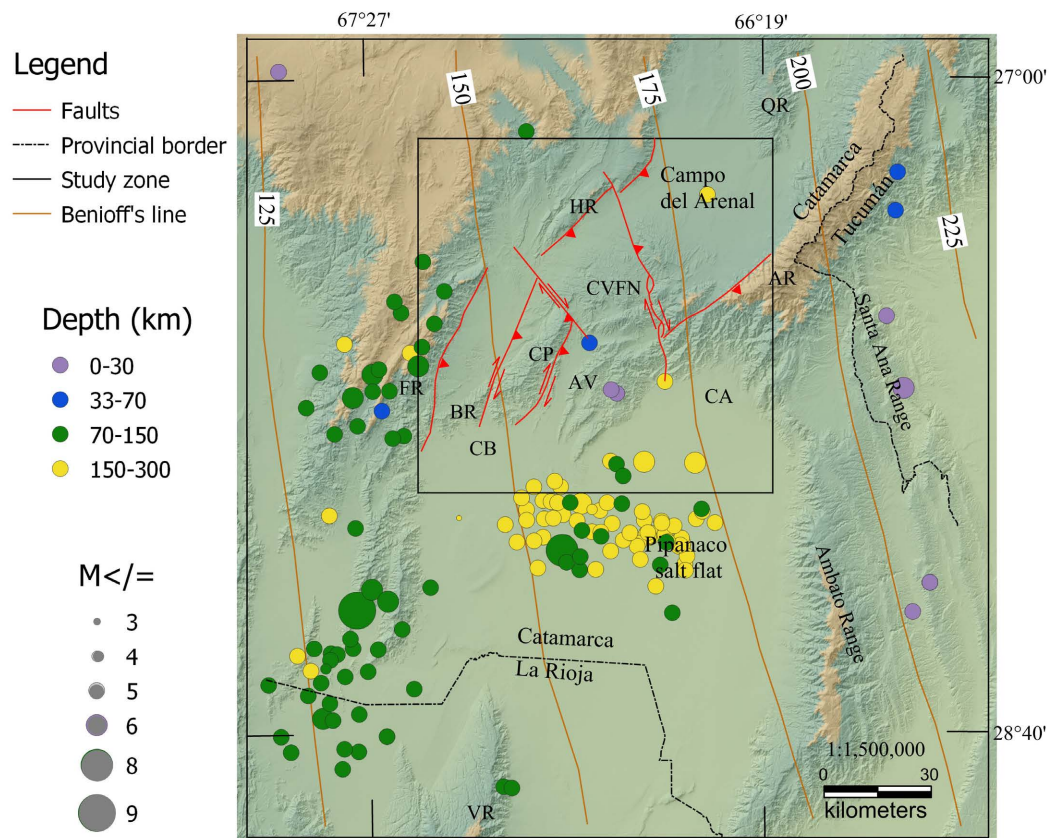


Figure 2. Simplified geologic map showing the study area in the context of the Wadatti-Benioff plane's depth lines and the position of the seismic source points and their magnitudes. QR: Quilmes Range. AR: Aconquija Range. CVFN: Farallón Negro Volcanic Complex. FR: Fiambalá Range. CP: Cerro Pampa. BR: Belen Range. AV: Ampujaco Valley. CA: Campo de Andalgalá. CB: Campo de Belén. VR: Velazco Range. Red triangle: reverse fault. Red arrow: transcurrent fault.

The continental sector of South America, east of the Andes, is characterized by north-south shortening, possibly caused by a collision with the Caribbean plate, which would have initiated the Andean orocline in an east-west compression tectonic scheme [2]. The Andean orocline [3] is of the secondary type, involving both the crust and the lithospheric mantle [4], and is characterized to the north by a counterclockwise rotation of about 37° (Figure 1(a)) (the Perú orocline) and to the south by a clockwise rotation of about 29° (Figure 1(a)) (the Arica orocline), which would have begun in the Late Eocene because of the convergence of the Nazca and South American plates [4] [5] [6] [7]. Magnetostratigraphic and paleomagnetic data from Cretaceous and Neogene rocks in the transition zone between the Puna and the Sierras Pampeanas (Hualfín-Santa María) demonstrate a clockwise rotation pattern [8] [9]. Dextral strike-slip along the transition zone between the Puna and the Sierras Pampeanas is demonstrated by structural studies [10] [11] [12]; however, this transition was interpreted as counterclockwise when morphotectonic expressions and paleomagnetic data were considered [13] [14] [15]. The clockwise rotation pattern in northern Chile's Andes (Precordillera and Cordillera Frontal) extends up to 29° S, indi-

cating that the Incaic deformation, which began in the Paleogene, ends at this latitude [15].

From a spatial standpoint, the Sierras Pampeanas feature an extended morphology with an NNW strike, which contrasts sharply with the Andean chain's NS strike (Figure 1). At the Sierras Pampeanas, ranges with NS, NNW, and NNE strikes are separated by extensive sedimentary basins and mega fractures with dextral and sinistral horizontal displacement, resulting in a counterclockwise rotation of the smaller mountain ranges [13] [16] (Figure 1). The Ambato Block is a crustal element that experienced counterclockwise horizontal rotation of the mountain ranges and was displaced to the east by plate convergence in the Cenozoic, with its rotation center in the north, colliding against the Sierra de Aconquija [17] [18] [19].

Our research contributes to the knowledge of the neotectonic deformation of large mountainous blocks formed above shallowly inclined subduction zones and its relationship with intense magmatic activity (Figures 1-3). We demonstrate the counterclockwise rotation of this set of mountain ranges, which collided with the Sierra de Aconquija because of plate convergence and had to rotate counterclockwise to accommodate the deformation. The thermal weakening of the crust caused by magmatic ascent favored counterclockwise rotation. During this tectonomagmatic process, transcurrent faults with vertical displacement components were formed to accommodate range uplift, intramontane basins were formed, magmatism and associated minerals were produced, and alluvial fans were separated from their riverbeds.

The mountain ranges (Cerro Pampa, La Ovejería, del Venado, Talayacu, Carrizal, and Algarrobal) that we call the Ovejería Block are separated from the Sierra de Aconquija by the Atajo fault (Figure 3). During the evolution of the volcanic complex, the mineralized dikes were formed and oriented from NE to NW. Connecting some fluvial and sedimentary processes with typically associated geomorphs (for example, alluvial fans) is impossible because tectonic processes unlinked them.

2. Regional Geology

The Sierras Pampeanas is between 27° and 33°LS, where the Nazca plate sinks beneath the continent at low angles of 5° to 10° [20], reaching a length of around 750 km from the oceanic trench. The Nazca plate subducts at a greater angle north of 27°S [20], indicating a period of oblique convergence trending NE in the Cenozoic [21] (Figure 1). According to [22], the Sierras Pampeanas were separated from the Puna. The Pampean horizontal subduction zone is most likely caused by two simultaneous collisions of aseismic mid-ocean ridges; the Copiapó ridge could control the northern limit of the flat subduction zone, while the Juan Fernandez ridge controls the southern boundary [23] (Figure 1).

The interaction of the Nazca plate has been linked to the deformation of the Andean foreland and the counterclockwise rotation of the Sierras Pampeanas

the Nazca plate beneath the South American plate during the Miocene exhumed igneous-metamorphic basement blocks in the Andean foreland, where the Sierras Pampeanas form through basement displacement involving high-angle reverse faults that likely cut through the entire crust [38] [39]. Previous research developed various models to link foreland deformation to the thermal structure and mechanical properties of the South American lithosphere [40], the geometry of subducted plates [10] [41] [42], and previous stratigraphic and structural inhomogeneities [43] [44].

The geological map of Capillitas [45] includes the research area. The Suncho Formation's metamorphic rocks, which date from the Late Precambrian to Early Cambrian, are the oldest [46]. In the Late Ordovician to Early Silurian, the widely dispersed Granito Capillitas rocks [47] intruded into the metamorphic rocks [48] [49]. A mylonitic zone about 1000 meters wide stretches along the eastern edge of the Atajo fault from Cerro Atajo to the Amanaos range in the south [50] (**Figure 3**). Northwest of Cerro Atajo, the Atajo fault disposes metamorphic rocks over Cenozoic sedimentary strata. South of Cerro Atajo, the Las Vizcachas fault lays mylonitic rocks upon metamorphic rocks [51] (**Figure 3**). The granitic and metamorphic rocks are discordantly overlain by Paleogene continental sedimentary rocks that were intruded by Farallón Negro Volcanic Complex rocks [47], on which Neogene continental sediments were later deposited [45] [47] [52] [53] (**Figure 3**). The Farallón Negro Volcanic Complex's dominant extrusive rocks are volcanic-tuffaceous andesitic breccias (purple and polymictic breccias) composed of poorly stratified dacitic and basaltic hornblende-pyroxene andesite breccias with a grey, violet-grey, or greenish-grey matrix [52].

Intrusive rocks and dike swarms have specific names (Dacita Arroyo Alumbra, Andesita El Durazno, Diques Cerro El Durazno, Riolita Las Casitas, Andesita La Chilca, Diques El Águila, Dacita Agua Tapada, Riodacita Macho Muerto, and Riolita Los Leones) based on their specific characteristics and emplacement age, dated by $40\text{ Ar}/39\text{ Ar}$ methods between 12.56 Ma and 5.9 Ma [54] [55].

A detailed analysis of the stratigraphy and geometry of the Cenozoic sedimentary basins of the surrounding region was carried out [56]. They interpreted that the initial Paleogene fill, comprising the Hualfín and Saladillo formations, appears associated with asymmetric depocenters controlled by normal faults. The El Morterito Formation is like the Calchaquense-Araucanense Formation and is Miocene in age because of the presence of fossil vertebrates [57]. It was deposited on the igneous-metamorphic basement [49]. Red banks deposited by fluvial systems were included in the Hualfín Formation (Eocene - Early Miocene?) and primary clastic, volcanoclastic, and intercalated volcanic deposits in the Farallón Negro Volcanic Complex (Upper Miocene - Pliocene) [58]. On the eastern slope of Cerro Pampa, lacustrine deposits like the San José Formation (Miocene) that crop out in the Santa María Valley were found and characterized. While there is no evidence that the Paraná seaway flooded the promontory in

Argentina's Sierras Pampeanas during the Miocene, the period of climate change that resulted in lake deposit is possible [59]. The Ampujaco Valley and the southern end of the Venado range were characterized as having ancient alluvial fans offset by faults [60]. Conglomerates, gravels, and sands containing volcanic rock components and sandy and silty eolian deposits represent the Quaternary [56] [61]. On the western edge of the Velazco range, thick alluvial fans of the Las Cumbres Formation were discovered and attributed to the Early Pleistocene [62] [63] [64]. The presence of fossil dacipodid plates found in the lacustrine layers confirms the Pleistocene age of these deposits, which are correlatable with the conglomerates of the Guanchín Formation [64] in the Bolsón de Fiambalá [65] [66]. These northwestern Sierras Pampeanas conglomerates are associated with the apex of the ascent of mountain blocks such as the Punaschotter [61] [64]. The Las Cumbres Formation and the Guanchín Formation conglomerates can be associated with the Yasyamayo Formation conglomerates in the Santa Maria Valley [67], which range in age from 2.9 to 1.5 Ma [68] [69].

3. Tectonic Scheme

International research on the central Andes' morphotectonic evolution used various methods and data to develop regional shortening directions and kinematic models. Four successive Andean deformational events were determined for the region [70]. A model of the upper crust comprising diamond-shaped domains with differential horizontal displacements along their edges caused by NW and ENE shortening was proposed [71]. Changes toward shortening have been dated in the Puna between 9 Ma [72] and 4 to 1 Ma [73] and continue into the Pleistocene [25] [74]. The Eastern Cordillera's curved structures and vertical uplifts were attributed to NS-oriented stress components generated by oblique shortening during Miocene-Pliocene deformation [75]. Based on surface and subsurface studies, the decoupling surface from where the basement blocks of the eastern Andean edge rise on one or both of their flanks has been explained in a variety of ways that place it at depths of 25 km and 10 to 15 km [22] [76]-[80]. The deformation and uplift of the sierras most likely began around 13 Ma [24], with significant uplifts occurring in 7.6 - 6 - 4 - 2.97 - 0.6 Ma and after 630 BP [68] [81] [82] [83] [84] [85]. Since roughly 9 Ma, the Sierra de Aconquija has experienced similar uplift, ~4 - 5 km, and 6 - 8 km exhumation [86]. The evolution of the El Cajón-Campo del Arenal basin from an initially undeformed state as of 11 Ma was described by [87]. The basin's internal deformation began at 6 Ma, along with the exhumation of the northern Quilmes range. By the middle Pliocene, the Quilmes range's total uplift had separated the El Cajón-Campo del Arenal basin from the Santa Maria basin. The Farallón Negro Volcanic Complex (**Figure 3**) is located to the north of the studied area and is bordered to the east by the Atajo fault. It has an elliptical geometry with a major axis strike to the NW, and its current morphology is because of the collapse of a volcanic structure that reached a height of around 6 km [53]. The elliptical geometries of the

cartographic features of the Bajo La Alumbra deposit and the Cerro Galán volcanic caldera, according to [44], are related to Andean deformation and serve as kinematic indicators.

The earthquake focal mechanisms and fault geometries in the research area and neighboring regions indicate NE and NW significant stress orientation [10] [88] [89] [90] [91]. The presence of normal faults with strike-slip components in the Bajo La Alumbra deposit indicates NE extension before 6.75 Ma [55]. The dikes and subvolcanic intrusions of the Farallón Negro Volcanic Complex were deposited in a structured pattern with a preferential NE strike at the beginning of the volcanic activity. The later shift to an NW strike, between 8.59 and 5.0 Ma, because of deformation rotation in this direction resulted in the formation of porphyry copper and epithermal deposits [29]. In the Vis-Vis ravine, south of the La Ovejera range, a caldera-shaped structure was discovered, associated with the Miocene volcanism of the Farallón Negro mining district [92] (Figure 3). A folded belt 100 to 200 km wide that extends from the north end of the Precordillera to the Santa Bárbara System is limited by the Salta and Tucumán lineaments and evidence an NNE compression [30]. In this belt, the Neogene and Quaternary tectonic evolution of the Ampujaco valley, among others, was produced by the reactivation of preexisting structures [14].

4. Methods

The primary source of data and the fundamental work methodology comes from the interpretation of satellite images. The visual interpretation of ASTER (Advanced Spaceborne Thermal Emission and Reflection Radiometer) [93], LANDSAT (Satellite for ground monitoring), SENTINEL (Satellite missions of the European Space Agency), and SRTM (Topographical Radar) [94] [95] satellite images were used to analyze tectonic morphology and interpret morphotectonic processes. These photos were also used to create thematic cartography. The geometry of the morphology adopted by the mountains, the layout and geometry of the major faults and the lineaments, the geometries of the forms originated by the faults, the morphologies adopted by the products of the superficial processes, and their relations with the tectonic processes are interpreted. The morphotectonic features of the region might be analyzed, and tectonic deformation processes could be explained using these tools. They also functioned as a location for identifying kinematic indicators and measuring structures to describe the tectonic processes that produced the contemporary landscape. Field data were collected over several years during campaigns, generating 193 measurements of fractures and faults, 101 measurements of schistosity planes in metamorphic rocks, 27 measurements of stratification planes in Tertiary sedimentary rocks, 31 measurements of pseudo stratification planes in volcanic rocks, and 31 measurements of bedding planes in Quaternary conglomerates. These data were analyzed using the Stereonet v11 software [96] [97] to determine the most common population orientations that respond to a state of local effort.

5. Results

5.1. Current Morphotectonic Scheme

The NE strike compressive shortening associated with Andean tectonic movements [89] [90] acts on the morphological landscape dominated by the NS orientation. In the Sierras Pampeanas, continental deformation from north to south is associated with the Juan Fernandez Ridge [41] [98].

During the Cretaceous, extensional processes that created rift basins influenced the retro arc zone. Neogene and Quaternary tectonic activity in the study area may also have evolved by reactivating some previous structures associated with the Cretaceous rift, as in adjacent regions [19] [85]. The previously uplifted terrain favored the development of reverse faults, transcurrent faults, and magmatism [14]. In the northern part of the La Ovejería range, the Farallón Negro Volcanic Complex [52] formed between 12.5 and 5.1 Ma [55] (**Figure 3**).

A reverse fault uplifted the mountain on one of its edges during the Pliocene [22]. During the Quaternary, Andean compressive tectonics also produced extensive and transpressive processes that shaped current morphologies, segmented and redirected Andean tectonics, and modified the drainage networks [13] [17] [18] [19] [85] [99].

5.1.1. Morphostructure

The study area is between Sierra de Aconquija in the east and Sierra de Fiambalá in the west (**Figure 1** and **Figure 2**). To the north is the Hualfín-Las Cuevas ranges. It is bordered to the northeast by Campo del Arenal and to the south by the Belén, Andalgalá, and Pipanaco salt flats (**Figure 2** and **Figure 3**). The Fiambalá, Hualfín - Las Cuevas range tilt northwestward due to reverse fault displacement along their eastern edges and are separate from the study area by the Hualfín Valley (**Figure 3** and **Figure 4**). The Fiambalá range strikes the NNE and is separated from the Hualfín range by the Ampujaco dextral fault. The Hualfín and Las Cuevas range strike the NE; they are displaced by the Atajo dextral fault (**Figure 3** and **Figure 4**). The Hualfín Valley extends southwards between the Fiambalá and Cerro Pampa and between the Belén range and Cerro Pampa (**Figure 3** and **Figure 4**).

1) *Ranges and hills*: The Atajo fault is a regional structure that falls on morpho-structural units that suffered deformation during Andean tectonism. The ranges to the east of the Atajo fault form the southern foothills of the Sierra de Aconquija (Cerros Atajo and Huyaco and the Capillitas, Santa Barbara, Yacochuyo, and Amanao ranges) (**Figure 4**). The Cerro El Durazno is a remnant promontory of the Farallón Negro volcano's cone, which was cut by the Atajo's fault. Scars on the Cerro Atajo show the sliding and collapse of its SW flank, which accounts for at least 1/4 of its surface. Cerro Huayco has a triangular morphology, with the western side connecting to the eastern edge of the La Ovejería range (**Figure 3** and **Figure 4**).

The Ovejería Block and the Farallón Negro Volcanic Complex are west of the

long, and the Algarrobal range is about 22 km long. The Carrizal and Algarrobal ranges and Quemado Hill form a block of NE strike made of granitic rocks about 40.5 km long and 14 km wide (**Figure 3**).

2) *Valleys and fields*. The Ampujaco valley extends with an NNE strike between the Venado range to the east and the Cerro Pampa to the west; at its widest point, it reaches 8 km in length (**Figure 5(a)**). This valley connects to the narrower Suncho valley to the north, which strikes E-W and separates the Ovejería and Venado ranges, through which the Suncho River flows into the Ampujaco valley (**Figure 3**, **Figure 4**, and **Figure 5(a)**).

The Tampa-Tampa (to the north) and Vis-Vis (to the south) fields are located on the western edge of the Atajo fault and occupy areas of 8.6 km² and 6 km², respectively. These fields were identified as caldera structures associated with mineralized zones [52] [91] [92] (**Figure 3** and **Figure 4**).

3) *Alluvial fans of the Ampujaco Valley*. On the eastern flank of Cerro Pampa, alluvial fans have distinct morphologic characteristics that distinguish them from others nearby. They were identified as the second level of the area (**Figure 5(a)**). Half-buried remains of alluvial fans, between 4 and 6 km long and up to 2 km wide, can be found to the south of the Ampujaco river valley, similar to those found on Cerro Pampa's eastern flank (**Figure 3** and **Figure 5(a)**). One of these piedmont deposits (**Figure 5(a)**) comprises sandstone from the base to the top, with intercalated lenticular conglomerates and matrix support. Passes into finely stratified conglomerates near the top, with a predominance of metamorphic, granitic, and volcanic clasts. The distal zone of the fan was eroded, leaving 5-meter-thick terraced levels.

This deposit is covered laterally by poorly sorted conglomerate facies, load-bearing clast with a fine matrix, and gravel-sized clasts of granitic, metamorphic, and scarcely volcanic composition; the blocks are more significant. Currently, the morpho-structural landscape of the Sierras Pampeanas is represented by mountain ranges and blocks, which are divided into smaller mountains with different orientations, sub-angular, approximately 50 cm in diameter, and predominantly granitic, compared to the underlying fan. The conglomerate disappears in the distal zone, to the north, beneath a stratified conglomerate at the base (35°NW dip), in contact with the Paleogene sediments (very cohesive orange-brown sandstones with a 58°W dip of the strata) (**Figure 6(a)**).

There is a sedimentary sequence about 11 meters thick, of stratified greenish-yellowish pellets (35°NW dip), with concretions (**Figure 6(b)**), south of the outcrops in **Figure 5(a)**, below the cenoglomeratic-conglomeratic sequence, which can be correlated with the San José Formation [100] of the Santa Maria Valley because of their lacustrine characteristics [60].

We can interpret from the various dips of these sedimentary units that a blind reverse fault, which is verging to the east, produced the plunge to the west on the geomorphic surface of the terraced levels of the alluvial fans (**Figure 6(c)**).

4) *Alluvial fans of the Algarrobal range*. An alluvial fan with a surface area of

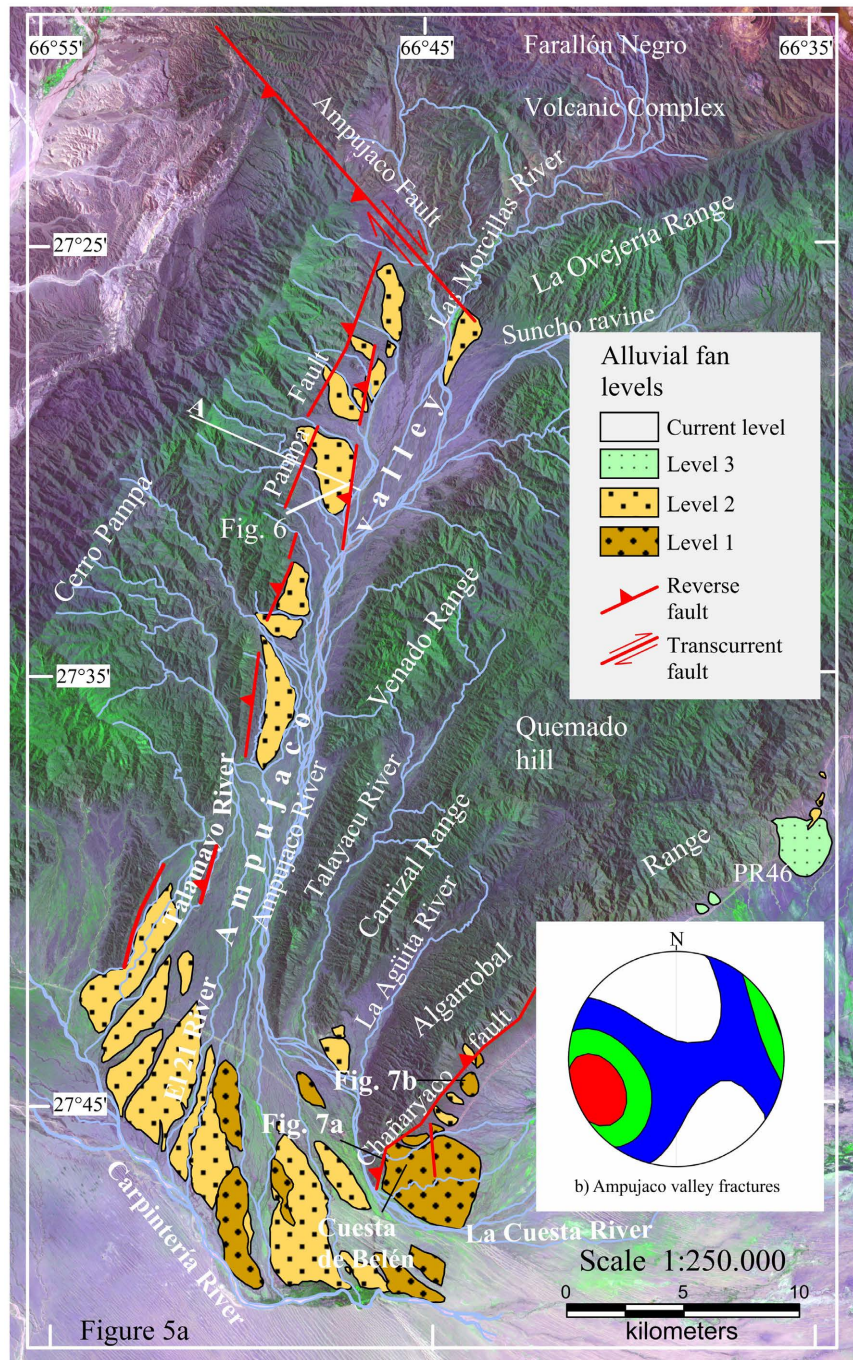


Figure 5. (a) Map showing the distribution of the alluvial fans in the Ampujaco valley and the eastern edge of the Algarrobal range. It is possible to distinguish four levels of the alluvial fan. The location of **Figure 6** and **Figure 7** are indicated on the map. A: Profil line. (b) Statistical diagrams of the fractures and faults poles in Schmidt's equiareal network, lower hemisphere. These fractures were measured in the Ampujaco valley. Colors reflect pole density; red: higher density. PR46: Provincial route N° 46. In **Figure 7** location, neotectonic faults are generated in the foothills, and these faults raise the tectonic morphology of the alluvial fans. The new faults have a different orientation and dip than the Chañaryaco fault and are generated far from the main fault (see details in **Figure 7(a)**). The Chañaryaco reverse fault disposes of the conglomeratic layers with a dip to the NE (see detail in **Figure 7(b)**).

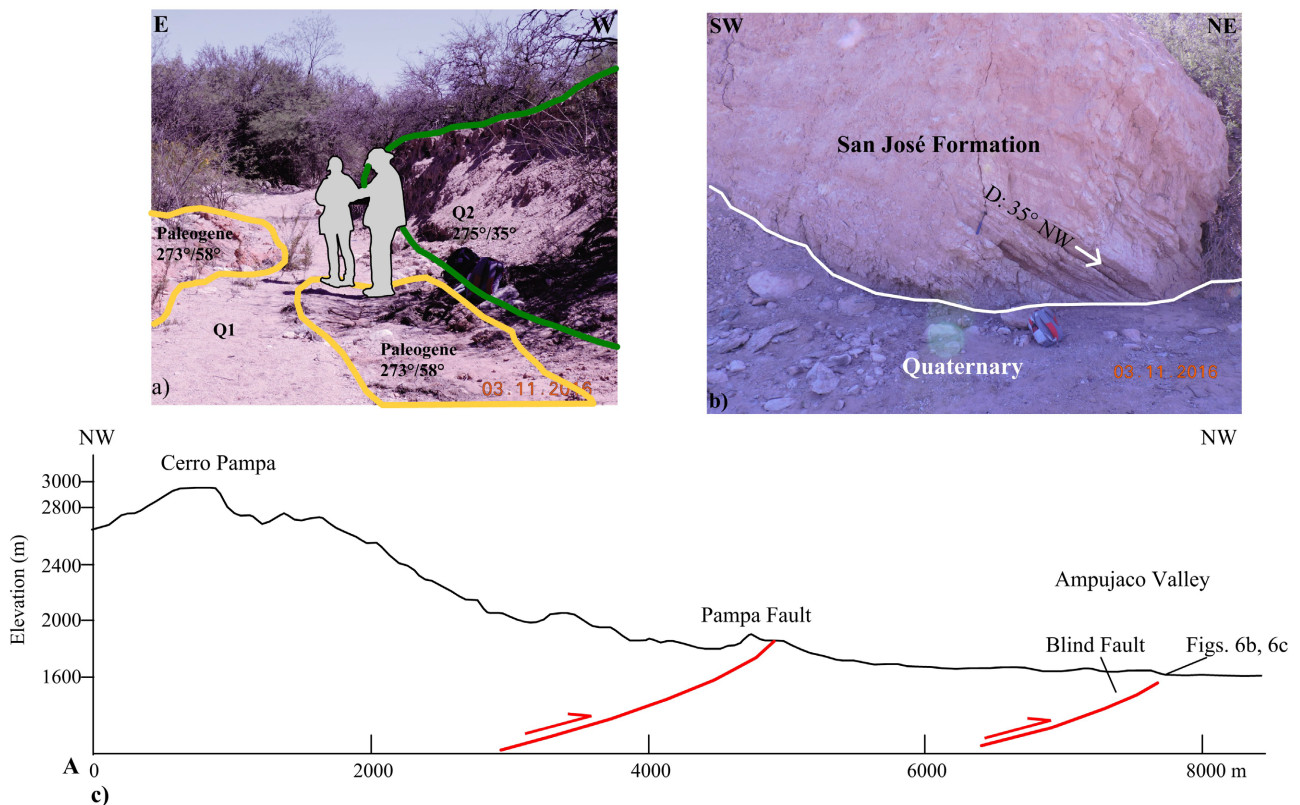


Figure 6. Location in **Figure 5**. (a) The reactivated external fault is blind, but it is evident because it affects Paleogene sedimentary rocks, reddish-brown color (DDD, 273°/58°) and consolidated Quaternary conglomerate (Q2: DDD, 275°/35°). Q1: fluvial sediments and Quaternary terrace deposits. (b) San José Formation, Neogene (35° NW dip) affected by the blind fault. (c) Topographic profile to show the Pampa faults and another blind fault in the foothills that provides for the westward dip of alluvial fan deposits and Paleogene sediments. Green line: geological contact.

12,500 m² is represented by a geform with an E-W strike at the southeast end of the Algarrobal range; the fan's apex is at the height of approximately 1200 m a.s.l. and is partially impacted by the Chañaryaco reverse fault (**Figure 3** and **Figure 5(a)**). The northern end of the deposit, which corresponds to Level 1 of the regional alluvial fans, is crossed by the Cuesta de Belén (PR46) (**Figure 5(a)**). The remains of alluvial fans like the one described and others that correspond to the second level can be seen to the north and along the same flank of the range (**Figure 5(a)**). The alluvial fan of the Cuesta de Belén has a typical morphology. It has a raised relief and a wavy geomorphologic surface dissected by the drainage network, indicating intense erosion. Faults divide the fans in the middle section to the north (**Figure 5(a)**). The fan mainly comprises conglomerate, generally well-selected and cohesive, load-bearing clasts, gravel-sized and isolated blocks up to 1.5 meters in diameter. The matrix is sparse near the foothills and more abundant in the distal and lateral facies; bedding is tabular parallel (DDD, 095°/55°), sloping towards the base and nearly horizontal towards the top (**Figure 7(a)**). The clasts are rounded to subrounded in shape, spherical, subprismatic, and discoidal in shape. They comprise lithic fragments of grey and pink granite, porous volcanic, and a few metamorphic clasts [60].

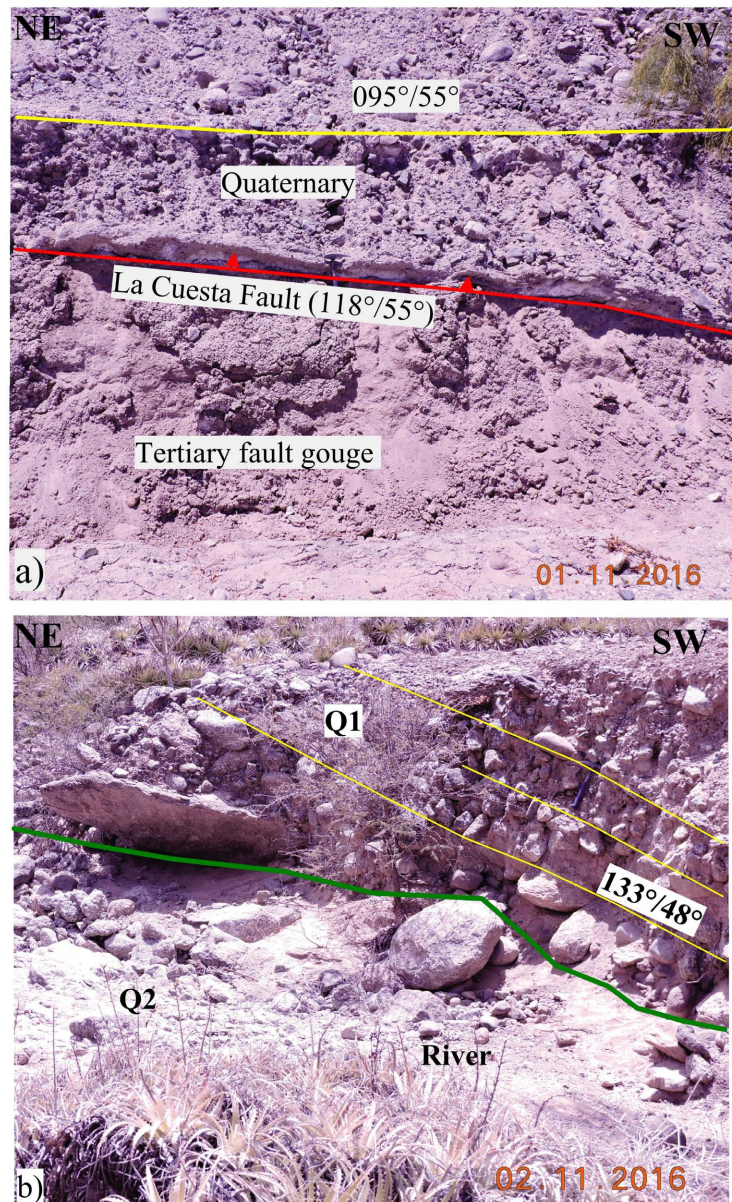


Figure 7. Location in **Figure 5(a)**. (a) Stratigraphic sequence that alternates between banks of thick, rounded conglomerates (the stratification is indicated by the yellow line: DDD, 095°/55°), with layers of coarse, brown, friable sandstone, with abundant sheets of gypsum. The reverse fault (indicated by the red line: DDD, 118°/55°) brings the sandbar into contact with the upper conglomerate bank. The fault plane is about 3 m thick. (b) View of the alluvial fan made up of rounded pebbles (the yellow line indicates the stratification: DDD, 133°/48°). The Chañaryaco reverse fault disposes of the conglomeratic layers with a dip to the SE. The conglomerates that form the alluvial fan are arranged on granite rock. The contact between the Quaternary deposits is indicated with a green line: Q1, conglomerates of the alluvial fan, older; Q2 river sediments.

Conglomerate deposits in some areas are on a granitic basement or in contact with undifferentiated Cenozoic rocks, such as brown, friable sandstones rich in gypsum (**Figure 7(a)**). A continuous level of fault breccia with a 118°/55° orientation (DDD), about 50 cm thick, is observed in the contact between the latter

(**Figure 7(a)**). Its surface geomorphology and conglomeratic composition differ significantly from the adjacent fans (Levels 3 and recent). Levels 3 and recent are modern alluvial deposits with a flat geomorphologic surface and rich sandy-silty supporting matrix (Herazo et al., 2017). An alluvial fan (Level 1) with smaller dimensions can be seen northeast of the Cuesta de Belén, but it is heavily consolidated on granite rock (**Figure 5(a)** and **Figure 7(b)**). This fan offsets the Chañaryaco reverse fault, which gives the conglomerate layers a solid tilt to the southeast (DDD, $133^{\circ}/48^{\circ}$) and is far from the mountain front (**Figure 5(a)** and **Figure 7(b)**).

The alluvial fans at the SE end of the Algarrobal range and the southern end of the Ampujaco River, which correspond to levels 1 and 2 (**Figure 5(a)**), are geomorphs unrelated to the elements that were necessary for their formation (such as the raised relief at its head, the source area of the materials, transport drainage, etc.), which managed to accumulate these volumes of rock that are currently strongly consolidated and in an advanced erosion stage. The alluvial fans described have a high relief, coarse granular composition, deep dissection from surface drainage, and are impacted by faulting. The younger alluvial fans (Level 3 and current level) (**Figure 5(a)**) have less dissected and fault-free reliefs, which starkly contrast with this. The age of the alluvial fans at Levels 1 and 2 is believed to be between the Pliocene and Pleistocene.

5.1.2. Structures

1) *Atajo fault*: The reverse vertical component of the Atajo fault, which has an NNW strike and measures about 69.5 km in length (**Figure 3**, **Figure 4**, and **Figure 8(a)**), dips 60° and 80° to the east. Granitic and mylonitic rocks are displaced over Cenozoic sedimentary rocks in the northwest region of Cerro Atajo and over volcanic rocks of the Farallón Negro Volcanic Complex (**Figure 3** and **Figure 9(a)**). The displacements between the Hualfín - Las Cuevas and La Ovejería - Cerro Huayco ranges (**Figure 3**, **Figure 4**, and **Figure 8(a)**) demonstrate that it also has a component of dextral horizontal movement.

According to [52] and [91] [92], the Tampa-Tampa and Vis-Vis basins are caldera structures with associated mineral deposits (**Figure 3**). We can interpret that displacement along the Atajo fault produced releasing and restraining bends by analyzing the geometry and morphology of the fault from satellite images, field data, and the morphologies of the Tampa-Tampa and Vis-Vis basins connected to mineralized zones (**Figure 8(a)**).

The Tampa-Tampa and Vis-Vis basins are linked to the releasing bend zones, while the western edge of Cerro Huayco is linked to the restraining bend zone (**Figure 8(a)**). Northwest of Cerro Atajo, on the northeast edge of the volcanic caldera, is where you will find the Tampa-Tampa field (**Figure 8(a)**). It is about 8.6 km^2 in size, and the faults overlap by about 4 km (**Figure 8(a)**). The Vis-Vis field, south of the La Ovejería range, is elongated, covers a surface area of 6 km^2 , and has faults that overlap by about 4.5 km (**Figure 8(a)**). The Atajo fault created a 4.2 km long restraining stopover between the edges of the La Ovejería

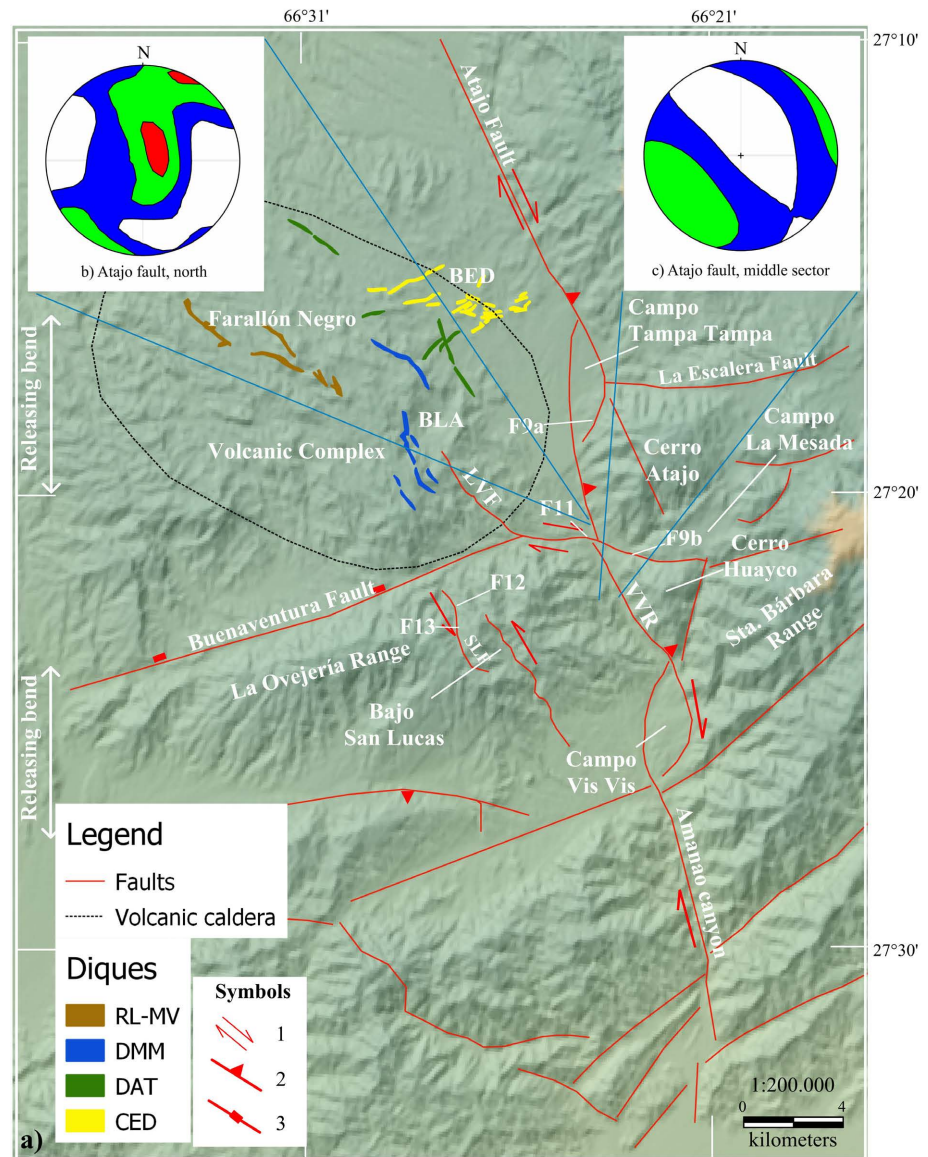


Figure 8. (a) Morphotectonic map of the study area. The regional structures, the volcanic caldera, the mineralized dikes with different orientations, and the main mountain ranges are shown. F9a: **Figure 9(a)** location. F9b: **Figure 9(b)** location. F10: **Figure 10** location. F11: **Figure 11** location. 1: Transcurrent fault. 2: Reverse fault. 3: Normal fault. BED: Bajo El Durazno. BLA: Bajo La Alumbreira. VVR: Vis-Vis River. SLF: San Lucas Fault. LVF: Las Vizcachas Fault. Mineralized dikes: RL-MV: Los Leones Rhyolite and mineralized veins (5 Ma). DMM: Dacita Macho Muerto (5.95 - 6.14 Ma). DAT: Agua Tapada Dacite (7.39 Ma). CED: Cerro El Durazno (8.10 - 8.59 Ma). (b) and (c) Statistical diagrams of geological fractures and faults poles in Schmidt's equiareal network, lower hemisphere. Colors reflect pole density; red: higher density.

range and Cerro Huayco (**Figure 8(a)**). The La Ovejería range included the Cerro Huayco. To make the dextral displacement of the Cerro Huayco, the Atajo fault split the northeastern end of the La Ovejería range, tilting the regional foliation in the metamorphic rocks that make them up towards the west, in the La Ovejería range, and to the east, in the Cerro Huayco (**Figure 3** and **Figure 8(a)**).

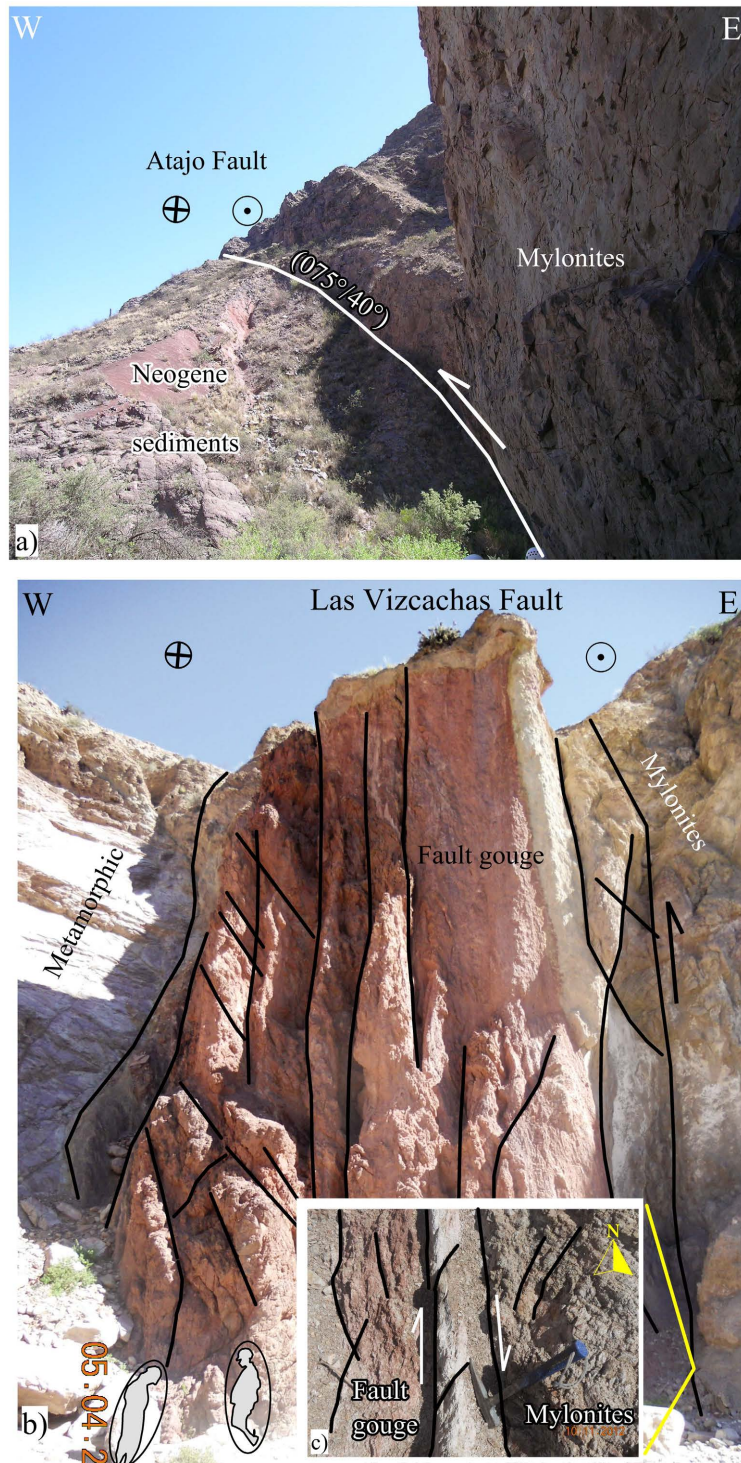


Figure 9. Location in **Figure 8** and **Figure 10**. Photographs illustrating the vertical and transcurrent behavior of the Atajo and Las Vizcachas fault. The dotted and cross circles indicate the dextral horizontal movement of the fault. The shape of people is the scale of the outcrop. (a) Granitic rocks thrust on Neogene sediments through the Atajo fault. (b) Mylonitic rocks thrust on metamorphic rocks along the Las Vizcachas fault. The thickness of the fault gouge is observed. (c) Image from the lower right corner of figure (b); secondary conjugate fractures are observed showing dextral horizontal displacement of the fault.

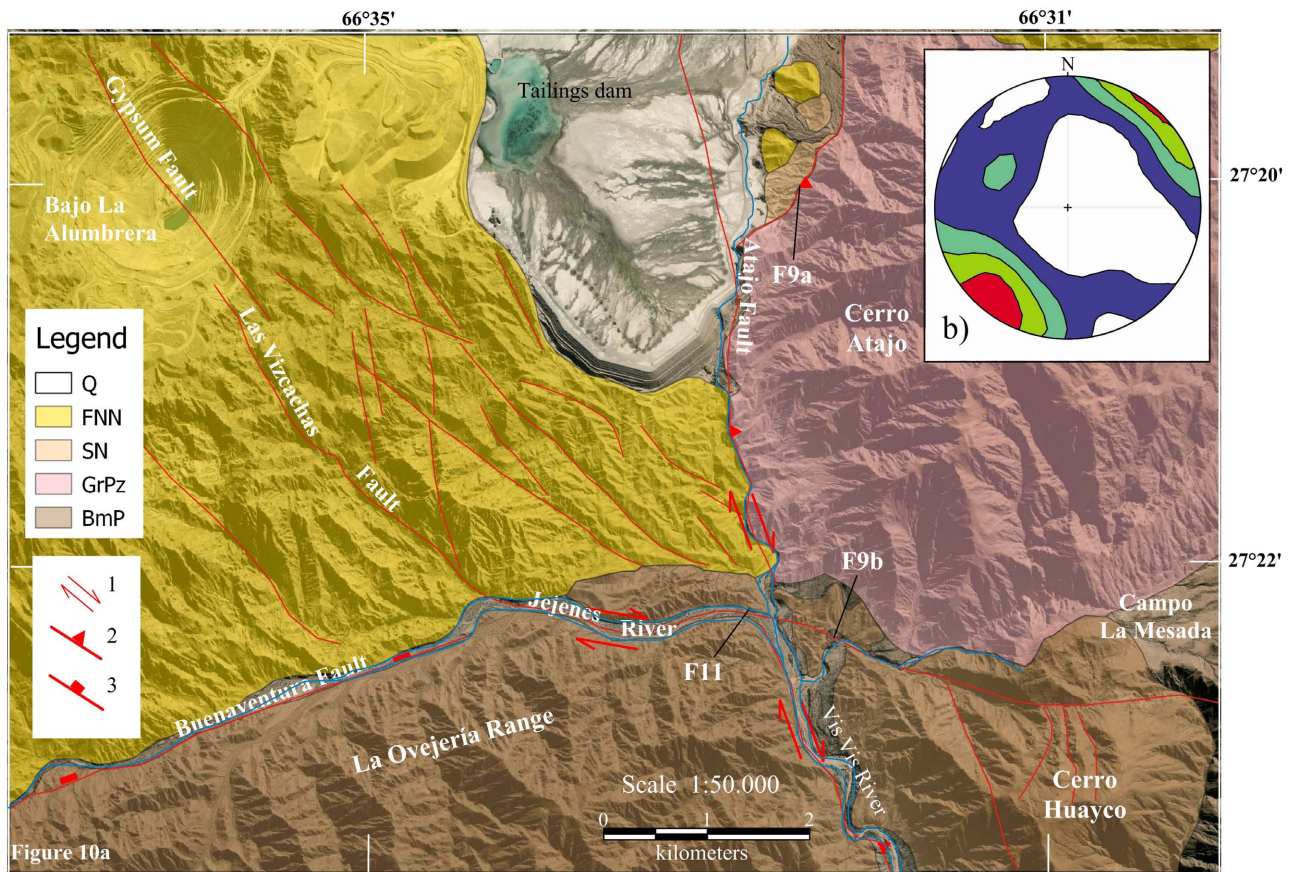


Figure 10. (a) Structural diagram of the Las Vizcachas fault zone. The fault cuts the northern edge of Cerro Huayco and La Ovejera range and then enters the volcanic caldera of Farallón Negro. Q: Quaternary. FNN: Farallón Negro Volcanic Complex, Neogene. SN: Sedimentary, Neogene. GrPz: Granite, Paleozoic. BmP: Metamorphic basement, Proterozoic. 1: Transcurrent fault. 2: Reverse fault. 3: Normal fault. F9a: **Figure 9(a)** location. F9b: **Figure 9(b)** location. F11: **Figure 11** location. (b) Statistical diagrams of geological fractures and faults poles in Schmidt's equiareal net, lower hemisphere. Colors reflect pole density; red: higher density.

The Farallón Negro Volcanic Complex's eastern boundary is also divided by the Atajo fault, and the Cerro El Durazno is a volcanic cone remnant of the NE. The measured fault planes on the Atajo fault strikes to the NW and NNW, respectively, west of the Cerro Atajo and Cerro Huayco, indicating a close relationship with the main trace of the fault and its geometry (**Figures 8(a)-(c)**). The Atajo fault would have been vital in causing the volcanic caldera to collapse (**Figure 8(a)**).

2) *Las Vizcachas fault*: The Las Vizcachas fault measures roughly 15 km (**Figure 8(a)** and **Figure 10(a)**). The fault occupies the central zone approximately 3 km wide, where other structures have the same strike on its side (**Figure 10(a)**). The stereonet software represented 27 measurements of the fault zone in Schmidt's net, lower hemisphere [95] [96] (**Figure 10(b)**).

Satellite images clearly show the curved nature of this fault, as well as its general NW strike and dextral horizontal displacement. It forms the boundary between Cerro Atajo and Cerro Huayco to the east (**Figure 9(b)**). It enters the Farallón

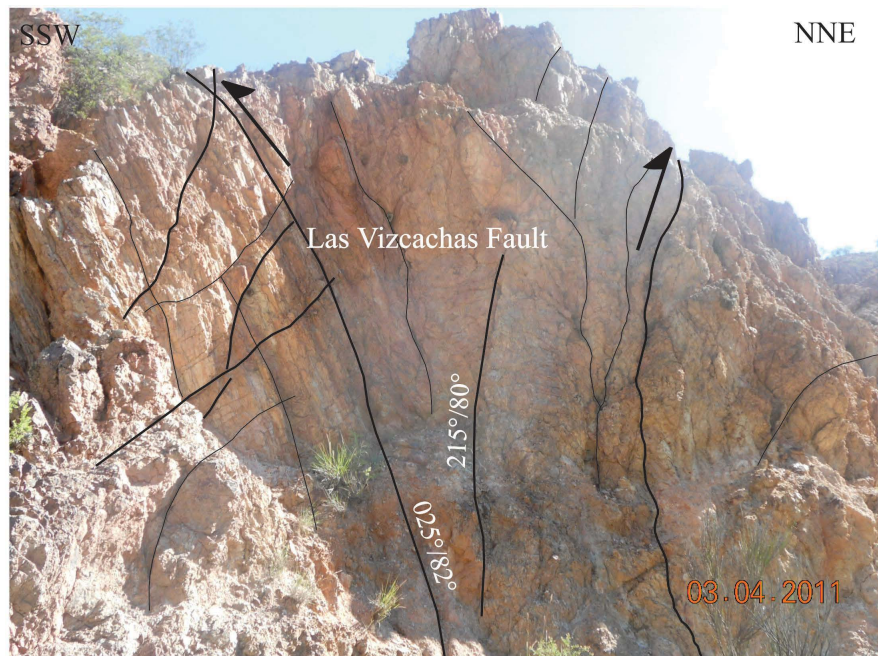


Figure 11. Positive flower structure of the Las Vizcachas dextral fault.

Negro volcano's caldera to the northwest, offsetting and cutting the Atajo fault (**Figure 8(a)**, **Figure 9(c)**, and **Figure 10(a)**). The secondary conjugate structures accompanying it confirm de dextral horizontal displacement (**Figure 9(c)**).

There are zones of both transtension and transpression in the horizontal shear zones. "Palm tree structures" are typically compressional structures with convex geometry [101]. The fault also caused the NE end of the La Ovejería range to split apart, creating a narrow valley home to the Jejenes river and only 3 km long and 180 m wide (**Figure 10(a)**). The field's most definitive evidence is the positive flower geometry produced in the metamorphic rocks (**Figure 11**).

3) *Buenaventura fault*: The Buenaventura fault, which has a normal displacement and dips 70° to the NNW [101], limits the La Ovejería range to the north (**Figure 4**, **Figure 8(a)**, and **Figure 10(a)**). Little evidence of displacement of the fault plane was found in the outcrops, but in the MW23 well located to the north of it, the basement was found in the subsoil at a depth of 128 m, indicating the dip and character of the surface of the fault [102].

4) *San Lucas fault*: The San Lucas fault, which is 7 km long, strikes NW, exhibits sinistral displacement, and creates a small pull-apart basin that is 1.14 km² in size. The basin has an elliptical shape, a 1.7 km length, and a major axis that strikes NW (**Figure 8(a)**). This depression contains subvolcanic intrusive rocks from the Farallón Negro Volcanic Complex [52], which broke through the igneous-metamorphic basement (**Figure 3** and **Figure 8(a)**).

Metamorphic rocks on the western side of the San Lucas fault display a fault plane (DDD: 267°/52°) (**Figure 12(a)**) and striations (DDD: 198°/05°) (**Figure 12(b)**) that are composed of horizontal displacement. The measured fracture planes in the region preferentially strike in the direction of the San Lucas fault,

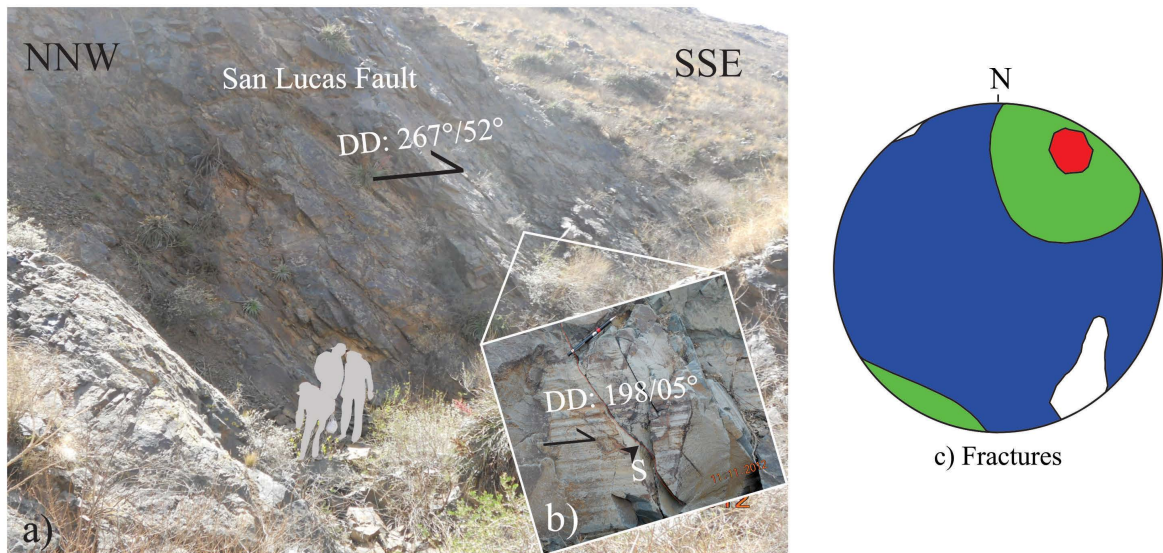


Figure 12. See location in **Figure 8**. (a) Field image of the San Lucas fault, carved in metamorphic rocks. (b) Striations of the fault plane defining horizontal displacement. **S** (secondary conjugate fracture) is indicated in the red line. (c) Lower hemisphere equal area projections of the fractures and faults poles. Colors reflect pole density; red: higher density. The shape of the people is a reference scale for the outcrop.

which is to the NW (**Figure 8(a)** and **Figure 12(c)**). Secondary conjugate fractures are also identified (**Figure 12(b)**), supporting the claim that the fault has been displaced sinistrally. Normal faults in this area cut quartz veins in the metamorphic basement (**Figure 13**).

5) *Ampujaco fault*: This fault represents a linear tectonic feature with an NW strike about 30 km long and can be seen in satellite images. It exhibits reverse vertical displacement components, an SW dip, and dextral horizontal displacement (**Figure 3** and **Figure 4**). Granitic rocks from Cerro Pampa are brought into contact with rocks from the Farallón Negro Volcanic Complex and metamorphic rocks from the La Ovejería range by this fault (**Figure 3**). It delineates the boundary between the Fiambalá and Hualfin ranges, which were displaced by this fault (**Figure 3** and **Figure 4**). At the northwest end of the La Ovejería range, the fault plane has an attitude of $240^{\circ}/80^{\circ}$ (DDD) (**Figure 3**).

6) *Belén fault*: This NE strike fault is 50 km long (**Figure 3** and **Figure 4**). The fault creates a small valley (8 km long) bordered to the west by the Belén range and to the east by the Cerro Pampa by dividing the southern sector of a mountainous block of granitic rocks (**Figure 3** and **Figure 4**). The valley widens towards the Belén field, where the town of Belén is situated and reaches a width of 3.20 km; to the north, it connects with the Hualfin valley, where the fault does not outcrop (**Figure 3** and **Figure 4**). This reverse fault dips to the west (DDD: $245^{\circ}/30^{\circ}$); at its northern end, it places granitic rocks on top of Neogene sediments (**Figure 14**).

7) *Pampa fault*: The fault limits the Ampujaco Valley's western boundary (**Figure 3** and **Figure 4**). It is a broken, 29 km-long reverse fault that lifts and tilts the Cerro Pampa to the west (**Figure 5(a)**). As another reverse fault that

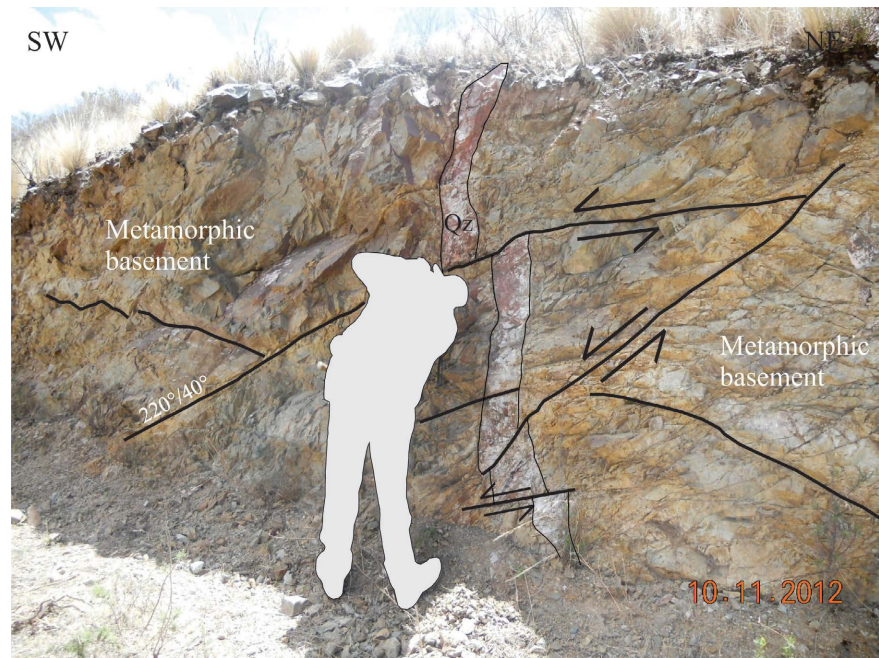


Figure 13. See location in **Figure 8**. Photo to show normal faults affecting metamorphic basement rocks. They are cutting and displacing a quartz vein.

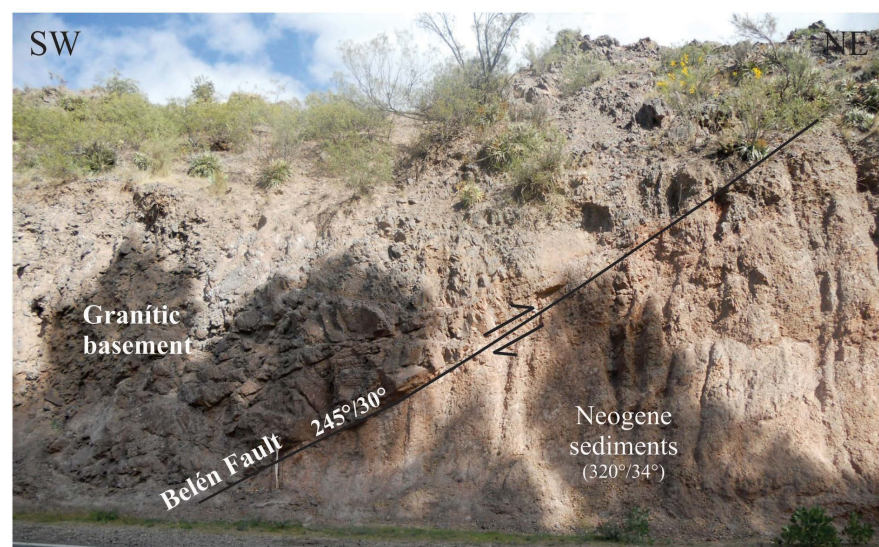


Figure 14. Outcrop on National Route 40. Location in **Figure 3**. The Belén fault (DDD, 245°/30°) produces the thrust of granite rocks over the Neogene sedimentary rocks. The general strike of the fault is NE, but in this area, it marks a break with an NW strike.

raises the stratification planes of Paleogene sedimentation that are orange-brown (DDD: 273°/58°) and the deposits of alluvial fans formed by highly consolidated conglomerates, possibly dating to the Early Pleistocene (DDD: 275°/35°), this fault's quaternary reactivation is visible 2.4 km to the east of the main fault (**Figure 5(a)** and **Figure 6**). These tectonic morphologies were described by [103] as outer faults, a byproduct of fault migration, creating a piedmont promontory between the two faults in tectonically active regions (**Figure 6(c)**). Some

fracture planes were measured on the western edge of the Ampujaco valley, indicating a preferential NNW strike (**Figure 5(b)**). Good examples of faults with various geometries created in the foothills because of the reactivation of earlier faults can be found in the Tafi valley [85].

8) *Chañaryaco fault*: The 39 km long fault strikes in the NE (**Figure 3** and **Figure 4**). Its morphotectonic expression is seen in the mountainous block of the Venado, Talayacu, Carrizal, and Algarrobal ranges, as well as Quemado hill, rising and tilting toward the west (**Figure 4**). Smaller structures limit the Talayacu, and Carrizal ranges on their eastern edge, tilting them to the west by verging to the east (**Figure 3** and **Figure 4**). Highly consolidated alluvial fan deposits, which make up Level 1 of these deposits in the foothills of this mountain block, east of the Chañaryaco fault, are being affected by normal and reverse structures of recent tectonic. These deposits are thought to date back to the Pliocene-Pleistocene (**Figure 7(a)**).

The reactivation of the Chañaryaco fault created these structures. Some have oblique orientations concerning the Chañaryaco fault's strike, with a generally NS strike and opposite dip directions (**Figure 7(a)**). The 1000-meter-long reverse fault La Cuesta (DDD: $118^{\circ}/55^{\circ}$) tilted the alluvial fan, separating it from the Algarrobal range and disposing of conglomerate layers with a strong dip to the east (DDD: $095^{\circ}/55^{\circ}$) and eroding it (**Figure 5(a)** and **Figure 7(a)**). The fault occurs where the brown sandstone meets the conglomerate deposits that make up the alluvial fan (**Figure 7(b)**).

The reactivation of the Chañaryaco fault also caused the tilting to the east and dismemberment of another alluvial fan (Level 1, **Figure 5(a)**) to the north, where the flank of the Algarrobal range forms a strongly curved inlet, concave to the east (**Figure 5(a)** and **Figure 7(b)**). The height of the counter slope of one of these residual deposits, which reaches approximately 90 m, can be seen in the satellite image. This is the product of the fault's tilting, which resulted in the conglomerate strata having a strong SE dip (DDD: $133^{\circ}/48^{\circ}$) (**Figure 7(b)**).

5.1.3. Mineralized Dikes

The magmatic activity allowed the Farallón Negro Volcanic Complex to form near the end of the Tertiary, resulting in porphyry copper and epithermal deposits (**Figure 3**). The dikes and subvolcanic intrusives were emplaced in the volcanic complex along a structural pattern that had a NE preferential trend at the start of the volcanic activity (CED: 8.10 - 8.50 Ma) but later changed to an NW strike (DAT: 7.39 Ma; DMM: 5.95 - 6.14 Ma and RL-VM) [29] (**Figure 8(a)**).

The volcanic complex's internal fracturing also has a preferential NNW to NW trend (**Figure 8(b)**, **Figure 10(b)**). The Farallón Negro Volcanic Complex's tectonic-magmatic evolution was controlled by the counterclockwise rotation of the shortening axis [29].

5.2. Statistical Treatment of Structural Data

The statistical diagrams of faults and fractures are represented in **Figure 5(b)**

(corresponding to the Ampujaco valley), **Figure 8(b)** and **Figure 8(c)** (along the Atajo fault), **Figure 10(b)** (representing the zone of Las Vizcachas fault), and **Figure 12(c)** (corresponding to the San Lucas fault). In all cases, a preferential NW strike of the structures is observed.

Schistosity measurements were taken on the Atajo fault, on the Vis-Vis river-banks, primarily in the La Ovejera range and Cerro Huayco outcrops. The schistosity planes strike NW, dipping steeply to the NE and SW (**Figure 3** and **Figure 15(a)**).

The stratification planes of Tertiary and Quaternary rocks and the pseudo stratification planes of volcanic rocks were measured on the Atajo fault, on both banks of the Vis-Vis River, between the volcanic caldera's eastern edge and Cerro Atajo's western flank (**Figure 3**). Subhorizontal NW strike is recorded in all cases (**Figures 15(b)-(d)**).

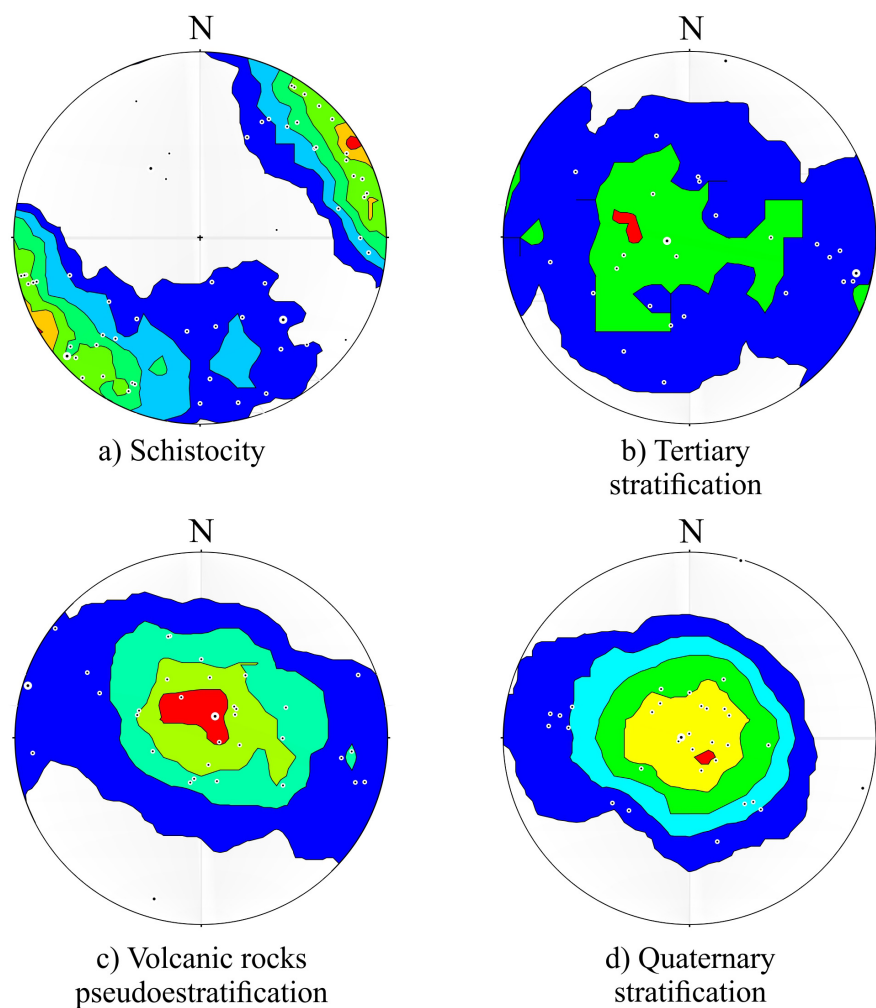


Figure 15. Statistical diagrams of the poles of the geological structure in Schmidt's equal-area network, lower hemisphere. Colors reflect pole density; red: higher density. (a) Schistosity planes of the metamorphic basement. (b) Stratification planes of Tertiary sedimentary rocks. (c) Planes of pseudo-stratification of volcanic rocks. (d) Quaternary deposit stratification planes.

5.3. Recent Tectonic Activity

We discovered neotectonic evidence in the Vis-Vis ravine, the Ampujaco valley, and the western edge of the Andalgalá field (**Figure 3** and **Figure 5(a)**). The deposits of terraced Quaternary alluvial fans were raised between 70 and 100 m above the level of the current river channel at the southern end of the Vis-Vis river's left bank, indicating the vertical reactivation of the Atajo fault (**Figure 3**). Some of these Quaternary terraces are affected by faults on the banks of rivers that drain into the Vis-Vis River, indicating recent tectonic activity (**Figure 16**).

The stratification of the Paleogene and Neogene sedimentary rocks (dipping 58°W and 35°NW , respectively) and Quaternary conglomerate deposits (dipping 35°NW) in the Ampujaco Valley (**Figure 6(a)** and **Figure 6(b)**) are all tilted to the west, revealing reverse and blind fault, verging to the east, in the distal zone of the alluvial fans (**Figure 5(a)** and **Figure 6(c)**).

Alluvial fan deposits are detached from the source area and a channel that feeds them on the eastern edge of the Algarrobal range (**Figure 5(a)**). Faults affect these deposits. The reverse fault La Cuesta (DDD: $118^{\circ}/55^{\circ}$) disposes of the stratification of the Cuesta de Belén alluvial fan with a 55° east dip (**Figure 5(a)** and **Figure 7(a)**). The reactivation of the Chañaryaco fault tilts towards the SE at an alluvial fan deposit (DDD: $133^{\circ}/48^{\circ}$) and separates it from the mountain front (**Figure 5(a)** and **Figure 7(b)**).

6. Discussion

6.1. Current Landscape

Numerous studies of the interaction of the Nazca and South American plates



Figure 16. Reverse fault in the quaternary sediment terrace on the right bank of the Huayco river.

show deformation of the Andean foreland as well as the displacement and rotation of the Sierras Pampeanas on a vertical axis [1] [13] [20] [24]-[30]. Also, the convergence of the Nazca and South American plates was attributed to the beginning of the rotation of the Andean orocline in the Late Eocene with counterclockwise about 37° north (Peru) and clockwise about 29° south (Arica) [4] [5] [6] [7] (**Figure 1(a)**). On the border between Puna and Sierras Pampeanas (Hualfin - Santa Maria) (**Figure 1(b)**), directly NW of the study area, magnetostratigraphic and paleomagnetic data from Cretaceous and Neogene rocks reveal a pattern of clockwise rotations [8] [9]. The upper, rigid part of the crust, which moves essentially in horizontal planes and elevates crustal blocks by one or both flanks, transmitted the compressional stress that gave rise to the Sierras Pampeanas, according to a variety of authors [22] [27] [76] [77] [78] [79] [80].

According to [16] [18] [19] [71] [104] [105] [106], the rheology of the rocks and pre-existing faults impact over deformation.

Other researchers postulate that the Andean foreland was impacted by NE compression and counterclockwise rotation. According to [2], the east of the Andes region of South America, which is affected by east-west compression, is characterized by north-south compression. Also, [14] demonstrate that stratigraphic units as recent as the Neogene, including the Precordillera, Sierras Pampeanas, Famatina System, Cordillera Oriental, and Santa Barbara System, folded because of the NNE shortening.

This research was based on interpreting regional tectonic morphology and evaluating structural data. Other studies revealed that some mountain ranges that make up the Sierras Pampeanas rotate counterclockwise [13] [16]. A crustal area affected by counterclockwise rotation because of plate convergence during the Cenozoic is the Ambato Block [17] [18] [19].

The study area is at the southern end of a curved mountain range made up of the Sierra de Aconquija and the Cumbres Calchaquíes, which have NNE strikes (**Figure 1**) and separate other mountain blocks with an NS strike (the Quilmes range to the north and the Ambato Block to the south) (**Figure 2**). The mountains that make up the study area also divide two significant sedimentary basins: the Pipanaco salt flat to the south and the Santa Maria valley-Campo del Arenal to the north (**Figure 2** and **Figure 3**). The elevated Hualfin valley, whose drainage network starts in the northeast of the town of Nacimientos de Arriba (**Figure 4**), travels through the Belén fault, and empties its waters into the Pipanaco salt flat, connecting these two intermontane depressions (Campo del Arenal and Pipanaco salt flat) (**Figure 4**). According to [60], the Ampujaco valley contains lacustrine sediments that are comparable to the San José Formation (Miocene), which could suggest a connection between the Santa Maria basins of Campo del Arenal, Hualfin Valley, and Pipanaco Salt Flat, possibly forming a larger basin in the early Cenozoic (**Figure 2** and **Figure 3**). According to [87], the uplift of the Quilmes range around 6 Ma because the uplift of the western edge of the Aconquija range caused the division and deformation of the El Cajón-Campo del Arenal basins.

A different geometry of the morphotectonic pattern can be seen when examining the study area in greater detail. The Atajo fault divides the southern portion of the mountainous complex of the study area to the west (Ovejería Block) and Sierra de Aconquija to the east (**Figure 3** and **Figure 4**). Three broken mountain blocks can be seen west of the Atajo fault; they are divided by the Ampujaco and Suncho valleys and comprise the Belén range-Cerro Pampa, Venado-Carrizal-Algarrobo, and La Ovejería ranges, with general NNE and ENE strikes, respectively. The north is bordered by a volcanic caldera (**Figure 3** and **Figure 4**).

The Atajo fault, in reverse slip sense with a NE dip and dextral displacement, produced two pull-apart basins (Tampa-Tampa and Vis-Vis fields) and the Cerro Huayco step-over, cut through the NE end of the Farallón Negro Volcanic Complex, and caused displacement between the Hualfín and Las Cuevas ranges and between the Ovejería Block and Sierra de Aconquija (**Figure 3**, **Figure 4**, **Figure 8**, and **Figure 9(a)**). Then, the Ovejería Block, which separates the southern end of the Sierra de Aconquija, rotated counterclockwise through the Atajo fault (**Figure 4**). Granitic and mylonitic rocks were juxtaposed on Cenozoic sedimentary rocks (**Figure 9(a)**), and the Atajo fault cuts the western edge of Cerro Atajo. The northern end of the La Ovejería range was separated and began rotating counterclockwise by the Atajo fault displacement, which also caused the Cerro Huayco to move, coinciding with the step-over geometry (**Figure 3** and **Figure 8**). The ranges El Durazno, Hualfín, Las Cuevas, Belén, and Aconquija deviated from the sub-meridional direction of the northern and southern ranges [107]. The regional shortening deviation to the NW near the end of the volcanic activity is explained by [55]. The orientation of the shortening variation from NE (8.10 Ma) to NNW (5 Ma) was interpreted by [13] and [29] based on the orientation of the sub-vertical dikes of the Farallón Negro Volcanic Complex (**Figure 8**).

The crust, including the Belén range, Cerro Pampa, has been cut by displacement along the Belén fault and rotated counterclockwise by the Pampa fault (**Figure 4** and **Figure 14**). The Ampujaco fault, with an NW strike and dextral displacement, terminates the northern edge of Cerro Pampa and separates it from the La Ovejería range (**Figure 3** and **Figure 4**). The Ampujaco and Suncho valleys were formed by the Cerro Pampa's counterclockwise rotation (**Figure 3** and **Figure 4**). Conglomerate deposits forming extensive alluvial fans (**Figures 5-7**) at the southern end of the Algarrobal range are devoid of a source area and drainage channels that fed them. This geological anomaly shows that the alluvial fan deposits were separated from their origins by a tectonic process (**Figure 3** and **Figure 5**). This can only be explained by a period before the mountains started rotating counterclockwise and the Ampujaco valley was formed. A single mountain block provided debris along transport channels for developing these piedmont deposits in a tectonically active area. Following the formation of the Ampujaco valley and the counterclockwise rotation of the crustal blocks, addi-

tional piedmont deposits would have accumulated on Cerro Pampa's western flank, creating at least three levels of piedmont deposits (**Figures 3-5**). The morphology of these piedmont deposits and the fault-tilted Quaternary terraces indicates recent tectonism (**Figure 6** and **Figure 7**).

Conglomerate deposits of the Pliocene-Pleistocene age were reported in the literature as Punaschotter. These conglomerates took their names from different places and were identified and described as Las Cumbres Formation, Guanchín Formation, and Yasyamayo Formation by [61]-[70].

The morphological and stratigraphic characteristics of the conglomerate deposits corresponding to Levels 1 and 2 alluvial fans in the Ampujaco Valley and Cuesta de Belén allow us to attribute them to Pliocene-Pleistocene age (**Figure 5** and **Figure 6**).

6.2. Origin of Counterclockwise Rotation

A concentration of seismic foci between 150 and 300 km depth is seen immediately north of the Pipanaco salt flat, along the 150 - 175 km depth lines of the Wadatti-Benioff zone [1] (**Figure 2**). In the study area, earthquakes with focal depths less than 30 km happen less frequently (**Figure 2**). During magmatic activity between 13 and 4 Ma, the Farallón Negro Volcanic Complex produced porphyry-type deposits of Cu-Au and epithermal Au (Mn, Ag, As, Pb, Zn) [54] (**Figure 3**). The Sierras Pampeanas would have developed a basal detachment between 10 and 15 km depth that was roughly horizontal because of the compression caused by the convergence of the Nazca and South American plates and the thermal weakening of the crust [22] [27] [76] [77] [78] [79] [80]. The crustal Ovejería Block could rotate counterclockwise under these circumstances (**Figure 17(a)** and **Figure 17(b)**).

The beginning of quartz's plasticity, or the brittle-ductile transition, occurs when the fault evolves and moves along deeper faults, as suggested by estimates of 10 - 15 km [31] [32]. Additional thermal input controlled by magma can cause this transition to occur at shallower levels. Still, it can also partially melt if the magma bodies have enough thermal energy. It has long been understood that partial melting that occurs as a network or in layers weakens rocks and can facilitate the initiation of faults [33]. Also, melting at grain boundaries weakens the rocks, and weak rocks deform more quickly [35]. Moreover, partial melts are channeled through increased deformation if the melt volume is large enough [34], which also supports the development of ductile shear zones [36] [37]. As a result, shear zones can form, and the middle crust deforms ductile, decreasing rock strength. Although the amount of melts produced by this process is significantly less than that of lower crustal levels, they should be able to support the initialization of ductile faults at levels > 25 km.

The size of the rigid block also affects how crustal rotations are related to faults and folds because of its presence in the fault path, according to experimental results. That this rigid block does not rotate when it is large and is instead cut by

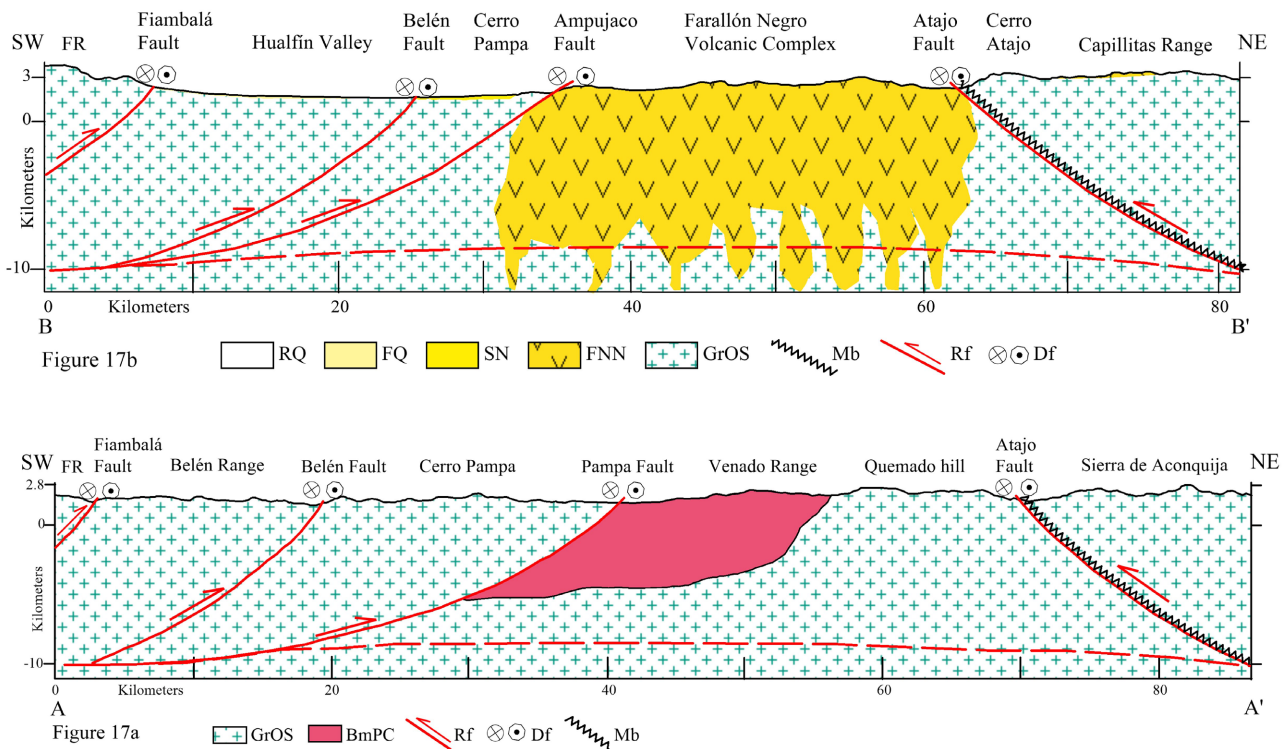


Figure 17. Note that, in both figures (a) and (b), the zone of crustal weakness, above which blocks experience counterclockwise rotation, coincides with the location of the metamorphic basement of the La Ovejera range and the Farallón Negro Volcanic Complex, between the Atajo, Pampa and Ampujaco faults (Figure 3 and Figure 4). The location of both profiles is in Figure 3. (a) Schematic crustal section showing the depth of the basal detachment. GrOS: Granito Capillitas, Upper Ordovician - Lower Silurian. BmPC: Metamorphic basement, Upper Precambrian - Lower Cambrian. Mb: Mylonitic belt. Rf: Reverse fault. Df: Dextral fault. (b) Schematic section showing the depth of the basal detachment. RQ: Recent sedimentary deposits. FQ: Foothill deposits, Quaternary. SN: Sedimentary rocks, Neogene. FNN: Farallón Negro Volcanic Complex, Neogene. GrOS: Granito Capillitas, Upper Ordovician - Lower Silurian. Mb: Mylonitic belt. Rf: Reverse fault. Df: Dextral fault.

strike-slip faults suggests that cutting the rigid block by faults is more straightforward and less energy-intensive than rotating the crust as a rigid block [108]. Even the formation of transcurrent structures with opposing kinematics is caused by the interposition of larger granitic bodies in the deformation trajectory [16].

To have a reference for their current position concerning the Sierra de Aconquija, the mountains west of the Atajo fault were divided into regions (Belén Ranges, Cerro Pampa, Ovejera, and Carrizal ranges) (Figure 18(a)). We propose a series of events that represent the tectonic morphology before the general uplift of the mountain ranges and any counterclockwise rotations, considering the current tectonic morphology, the geometry of the mountain ranges, and the structural relationships between them (Figure 18(b)).

The Ovejera Block region was rotated clockwise (Figure 18(a)), following the reverse path of deformation that produced the present landscape (Figure 4). The Belén, Cerro Pampa, Ovejera, and Carrizal ranges formed a chain with the same NE strike as the Sierra de Aconquija (Figure 18(a)) before the deposition of San José lacustrine sediments in the Ampujaco valley during the early Miocene. Likely,

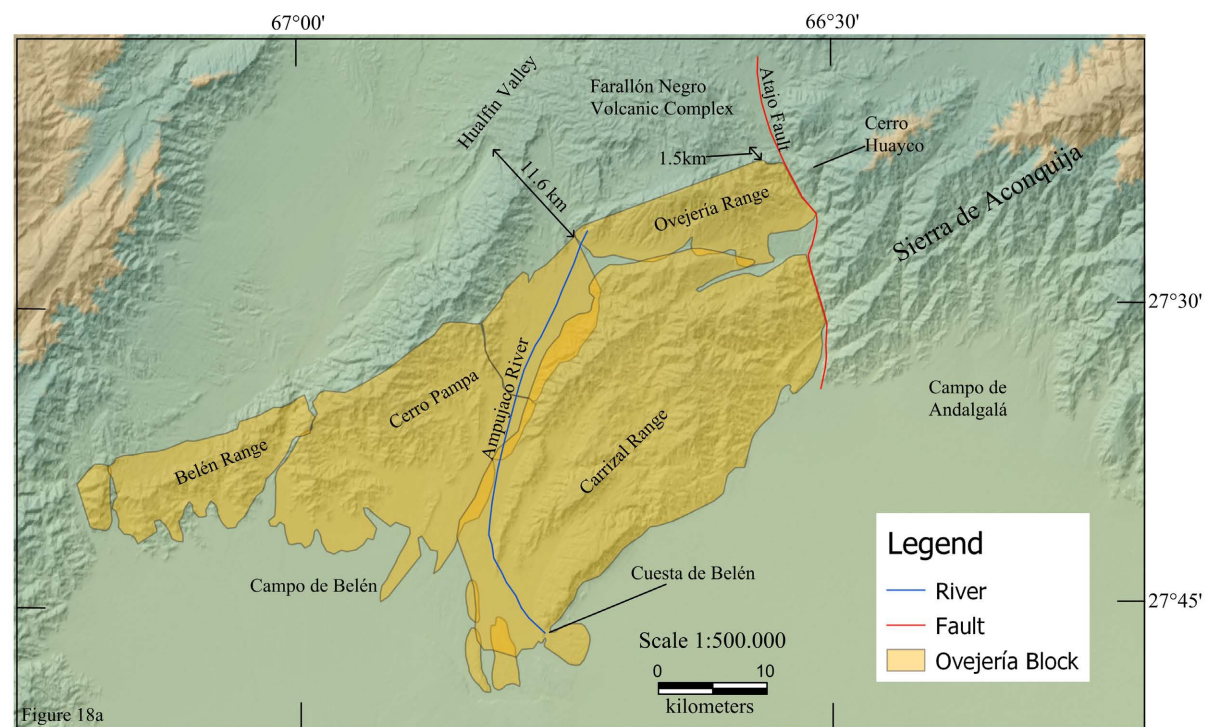
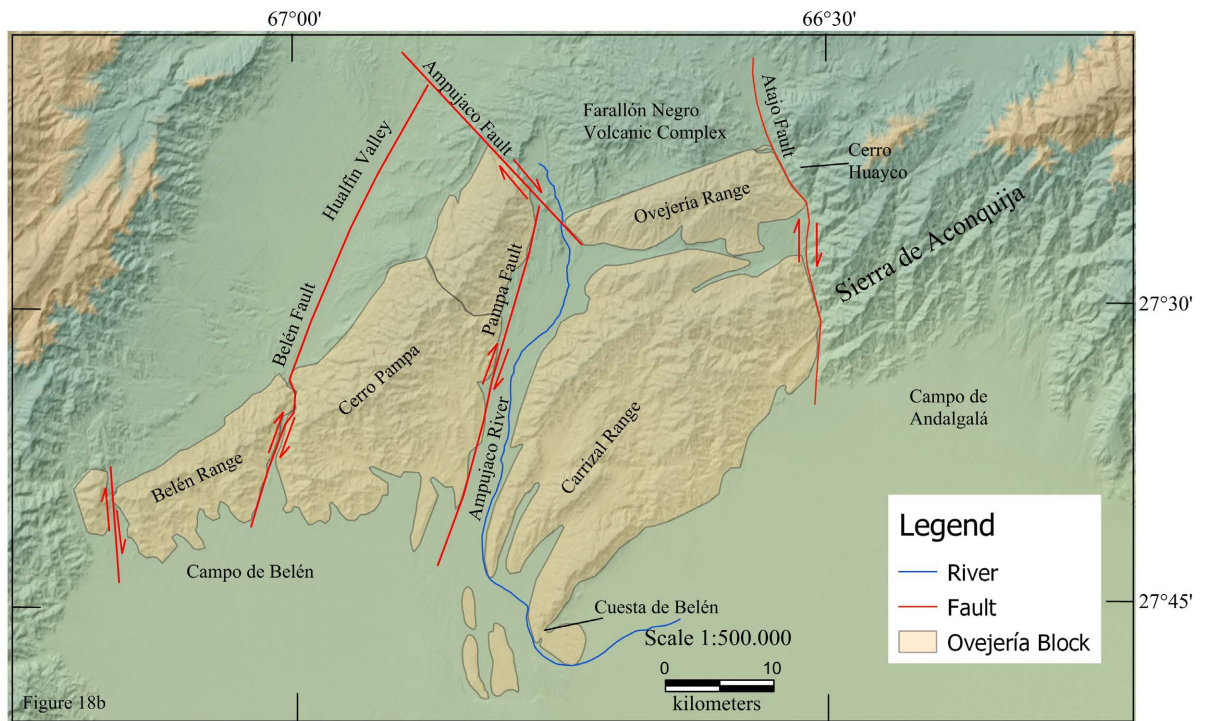


Figure 18. (a) Morphotectonic pattern at the beginning of the deformation, Paleogene. The alluvial fan of the Cuesta de Belén was deposited during the initial uplift of the Ovejería Block before the rotation of the ranges. The Atajo Fault existed before the raising and rotation of the Ovejería Block, marking the limit with the Sierra de Aconquija. Location and direction of runoff that the Ampujaco River would have had to deposit the conglomerates that formed the alluvial fan of the Cuesta de Belén. These alluvial fans contain rounded, granitic, and volcanic pebbles, which show a long journey whose origin could have coincided with the northern end of the Cerro Pampa and Ovejería Range. (b) Current morphotectonic pattern after counterclockwise rotation of the ranges.

the Santa Maria Valley, the Campo del Arenal, the Hualfin valley, and the Pipanaco salt flat were connected before the Miocene, forming a sizable basin broken up by low relief hills. In the southernmost portion of the Sierra de Aconquija, the Atajo fault would have already been a structural feature (**Figure 18(a)**). Also, some faults are likely inherited from the Cretaceous rift (**Figure 13**), which constrained depocenters that contained Paleogene sedimentary rocks [56].

The mountainous block comprised of the Sierra de Aconquija and Cumbres Calchaquíes, composed of granitic bodies with batholithic dimensions, is thought to have interacted with other mountainous blocks because it is rocky, rigid, and impassable massif. In the present instance, this rocky massif significantly influenced the rotation of the mountains in the study area counterclockwise. The Atajo fault bound the Sierra de Aconquija to the south, creating a positive element during the middle Miocene against which the Ovejería Block collided and rise (**Figure 18(a)**).

The counterclockwise rotation occurred through the horizontal dextral displacement of the Atajo, Pampa, Ampujaco, and Belén faults (**Figure 18(b)**).

At Farallón Negro, volcanic activity began at 13 Ma because of magmatic activity. The Cerro El Durazno dikes were deposited with a NE strike between 8.10 and 8.59 Ma, and the mineralized dikes associated with the intrusive Agua Tapada dacite were deposited with an NNW strike between 7.39 Ma and 7.39 Ma [54] [108] (**Figure 8(a)**). With a NE and NNW strike, these dikes show the beginning and evolution of the Ovejería Block's counterclockwise rotation. The Macho Muerto dacite dikes began between 5.95 and 6.14 Ma, with NW and WNW strikes [54] (**Figure 8(a)**). The Macho Muerto dacite dikes and the Las Vizcachas fault zone (**Figure 8(a)** and **Figure 10(a)**) share a similar NW strike, and both were formed between 5.95 and 6.14 Ma. The Los Leone's rhyolite intrusion gave rise to the mineralized dikes around 5 Ma, and the mineralized veins persisted in subsequent events, all with NW strike [54] [108] (**Figure 8(a)**).

The conglomerates of the Level 1 alluvial fan (**Figure 3** and **Figure 5(a)**) were deposited after these final subvolcanic intrusive rocks toward the end of the Pliocene and at the time of the most significant uplift of the mountain ranges that make up the Ovejería Block. After forming the Ampujaco and Suncho valleys and the end of counterclockwise rotation, the conglomerates of the Level 2 alluvial deposits (**Figure 5(a)**) were deposited during the Pleistocene.

The counterclockwise tectonic process of the mountains occurs on either side of the southern end of the Sierra de Aconquija. Ambato Block to SE [19] and Ovejería Block to SW of the Sierra de Aconquija (**Figure 18(b)**).

7. Conclusions

The Andean deformation caused by plate convergence is accommodated not only by E-W shortening but also by horizontal displacements caused by range rotation about a vertical axis and, sometimes, by NNE shortening. In the Lower Miocene, the Ovejería Block had a NE regional orientation, like the Sierra de

Aconquija orientation (**Figure 18(a)**). We propose that the Ovejería Block rotated counterclockwise because of the NE convergence of the Nazca and South American plates (**Figure 18(b)**). Displacement along the Atajo, Pampa, and Belén faults allowed for tectonism related to the mountain ranges' counterclockwise rotation (**Figure 18(b)**). This displacement of the rigid upper crust over the lower crust during the magmatic activity at 13 Ma was made possible by an enhanced geothermal gradient.

1) We interpret that in the early Cenozoic, the Santa Maria Valley, Campo del Arenal, Hualfin valley, and Pipanaco salt flat were linked and formed a large basin, which was broken up by hills with low relief. In this basin, lacustrine sediments, equivalent to the San José Formation, were deposited.

2) The uplift of the Sierra de Aconquija on the Ovejería Block through the Atajo fault started after the deposition of lacustrine sediments from the Lower Miocene. The mountain blocks rotated counterclockwise horizontally between 10 and 15 km depth (**Figure 17(a)** and **Figure 17(b)**). The Ovejería Block also started rotating counterclockwise.

3) The NE transpressive compression created the current landscape, which moved the Belén range and Cerro Pampa about 11.6 km to the NW and rotated them by about 20° counterclockwise (**Figure 18(a)** and **Figure 18(b)**). The La Ovejería range shifted to the NW by roughly 1.50 km (**Figure 18(a)** and **Figure 18(b)**). The Cerro Huayco, now east of the Atajo fault, was a portion of the La Ovejería range's eastern end (**Figure 10**, **Figure 18(a)**, and **Figure 18(b)**).

4) The thrusting of the Sierra de Aconquija on the Ovejería Block was caused by the Atajo fault, which in its geologic history displayed both ductile and brittle behavior (as shown by the mylonitic strip on its eastern edge). The Atajo fault exhibits dextral and reverse sense displacement with west vergence in its kinematics. Kinematics that produced pull-apart basins, including the Tampa-Tampa and Vis-Vis fields and a step-over on the western edge of Cerro Huayco, are recorded in the middle section of the Atajo fault (**Figure 8**).

5) The local rotation of the stress tensors in the study area, from NE to NW, between 13 and 5 Ma, was caused by the rotation of the Ovejería Block. The Farallón Negro Volcanic Complex's mineralized dikes, which date back to approximately 8.10 Ma in a NE strike and about 5.0 Ma in an NW strike, demonstrate the extent of the trans pressure caused by the rotation of the Ovejería Block (**Figure 8(a)**). The Macho Muerto dacite dikes were erected between approximately 6.14 and 5.95 Ma, according to the geometry of the Las Vizcacha fault zone (**Figure 8(a)** and **Figure 10**).

6) Our morphotectonic sequence includes the Cuesta de Belén's alluvial fan (**Figure 18(a)**). The Pliocene to Pleistocene age is when the alluvial fans were deposited, corresponding to Level 1 of the Cuesta de Belén. We believe that the Ampujaco River, whose supply basin was at the top of the Cerro Pampa and La Ovejería range, was responsible for depositing these alluvial fans (**Figure 18(a)**).

7) Through progressive deformation, the Belén range and Cerro Pampa un-

derwent further counterclockwise rotation, separating from the La Ovejería range to create the Ampujaco valley, where the Level 2 alluvial fans from the Pleistocene were deposited (**Figure 3**, **Figure 5**, and **Figure 18(b)**).

Acknowledgements

The National University of Tucumán, Minera La Alumbra, and the Argentine-German University Center contributed to support our research. We appreciate the reviewers' corrections, especially those made by Dr. John Geissman, who significantly improved the manuscript. We certify that the primary and processed data used in the research are kept and available at CONICET digital.

Conflicts of Interest

The authors declare no conflict of interest.

References

- [1] Yañez, G. and Ranero, C. (1999) The Role of the Juan Fernández Ridge in the Long-Lived Andean Segmentation at 33° S. *4th International Symposium on Andean Geodynamics*, Göttingen, 4-6 October 1999, 815-819.
- [2] Assumpcao, M. (1992) The Regional Intraplate Stress Field in South America. *Journal of Geophysical Research*, **97**, 11,889-11,903. <https://doi.org/10.1029/91JB01590>
- [3] Carey, S.W. (1955) The Orocline Concept in Geotectonic. *Proceedings of the Royal Society of Tasmania*, **89**, 255-288.
- [4] Johnston, S.T., Weil, A.B. and Gutiérrez-Alonso, G. (2013) Oroclines: Thick and Thin. *Geological Society of America Bulletin*, **125**, 643-663. <https://doi.org/10.1130/B30765.1>
- [5] Taylor, G., Grocott, J., Pope, A. and Randall, D. (1998) Mesozoic Fault Systems, Deformation, and Fault Block Rotation in the Andean Forearc: A Crustal-Scale Strike-Slip Duplex in the Coastal Cordillera of Northern Chile. *Tectonophysics*, **299**, 93-109. [https://doi.org/10.1016/S0040-1951\(98\)00200-5](https://doi.org/10.1016/S0040-1951(98)00200-5)
- [6] Coutand, I., Chauvin, A., Cobbold, P.R. and Gautier, P. (1999) Vertical Axis Rotations across the Puna Plateau (Northwestern Argentina) from Paleomagnetic Analysis of Cretaceous and Cenozoic Rocks. *Journal of Geophysical Research*, **104**, 22,965-22,984. <https://doi.org/10.1029/1999JB900148>
- [7] Arriagada, C., Roperch, P., Mpodozis, C. and Cobbold, P.R. (2008) Paleogene Building of the Bolivian Orocline: Tectonic Restoration of the Central Andes in 2-D Map View. *Tectonics*, **27**, TC6014. <https://doi.org/10.1029/2008TC002269>
- [8] Butler, R.F., Marshall, L.G., Drake, R.E. and Curtis, G.H. (1984) Magnetic Polarity Stratigraphy and 40K-40Ar Dating of the Late Miocene and Early Pliocene Continental Deposits. Catamarca Province. NW Argentina. *Journal Geology*, **92**, 623-636. <https://doi.org/10.1086/628902>
- [9] Aubry, L., Roperch, P., de Urreiztieta, M., Rossello, E. and Chauvin, A. (1996) Paleomagnetic Study along the Southeastern Edge of the Altiplano-Puna Plateau: Neogene Tectonic Rotations. *Journal of Geophysical Research*, **101**, 17,883-17,899. <https://doi.org/10.1029/96JB00807>
- [10] Jordan, T.E., Isacks, B.L., Allmendinger, R.W., Brewer, J.A., Ramos, V.A. and Ando,

- C.J. (1983) Andean Tectonics Related to Geometry of Subducted Nazca Plate. *Geological Society of America Bulletin*, **94**, 341-361.
[https://doi.org/10.1130/0016-7606\(1983\)94<341:ATRTGO>2.0.CO;2](https://doi.org/10.1130/0016-7606(1983)94<341:ATRTGO>2.0.CO;2)
- [11] Allmendinger, R.W. (1996) Tectonic Development, Southeast Border of the Puna Plateau, Northwest Argentine Andes. *Geological Society of America Bulletin*, **97**, 1070-1082. [https://doi.org/10.1130/0016-7606\(1986\)97<1070:TDSBOT>2.0.CO;2](https://doi.org/10.1130/0016-7606(1986)97<1070:TDSBOT>2.0.CO;2)
- [12] Urreiztieta, M. de, Rosello, E.A., Gapais, D., Le Corre, C. and Cobbold, P.R. (1993) Neogene Dextral Transpression at the Southern Edge of the Altiplano-Puna (NW Argentina). *2th International Symposium on Andean Geodynamics*, Oxford, 267-269.
- [13] Gutiérrez, A.A. (2000) Morphotectonic Evidence of Sinistral Rotation of the Pampeanas Mountain Ranges, Argentina. *17th Simposio Latinoamericano de Geología*, Stuttgart, Band 18, 6 p.
- [14] Gutiérrez, A.A. and Mon, R. (2017) Cuencas Cenozoicas contraccionales en los valles Ampujaco, Santa María y Río Nío, Argentina. *XX Congreso Geológico Argentino*, Tucumán, 132-139.
- [15] Peña Gómez, M.A. (2012) Reconocimiento del límite sur del patron Paleógeno de rotaciones horarias entre los 28°-32° S del margen Chileno a través de un estudio paleomagnético. Universidad de Chile, Facultad de Ciencias Físicas y matemáticas, departamento de Geología, Santiago de Chile, Memoria, 81 p.
- [16] Zampieri, D., Gutiérrez, A.A., Massironi, M. and Mon, R. (2012) Reconciling Opposite Strike-Slip Kinematics in the Transpressional Belt of the Sierra Pampeanas (Argentina). *European Geosciences Union General Assembly*, Vienna, 2 p.
- [17] Gutiérrez, A.A. (1999) Tectonic Geomorphology of the Ambato Block, (Northwestern Pampeanas Mountain Ranges, Argentina). *4th International Symposium on Andean Geodynamics*, Göttingen, 4-6 October 1999, 307-310.
- [18] Gutiérrez, A.A. and Mon, R. (2008) Macroindicadores cinemáticos en el Bloque Ambato, provincias de Tucumán y Catamarca. *Revista de la Asociación Geológica Argentina*, **63**, 24-27.
- [19] Gutiérrez, A.A., Mon, R., Arnous, A. and Cisterna, C.E. (2019) Sinistral Rotation and NNW Shortening of the Ambato Block Induced by Cenozoic NE to E-W Transpression, Argentina. *International Journal of Earth Science and Geology*, **1**, 74-85. <https://doi.org/10.18689/ijeg-1000109>
- [20] Isacks, B.L., Jordan, T., Allmendinger, R. and Ramos, V. (1982) La segmentación tectónica de los Andes Centrales y su relación con la geometría de la Placa de Nazca subductada. *V Congreso Latinoamericano de Geología*, Vol. 3, 587-606.
- [21] Cande, S. (1983) Nazca-South America Plate Interactions 80 m.y. B.P. to Present. *EOS*, **64**, 65 p.
- [22] González Bonorino, F. (1950) Algunos problemas geológicos de las Sierras Pampeanas. *Revista de la Asociación Geológica Argentina*, **5**, 81-110.
- [23] Álvarez, O., Giménez, M., Folguera, A., Spagnotto, S. and Braitenberg, C. (2014) La dorsal asísmica Copiapó y su relación con la cadena volcánica Ojos del Salado-San Buenaventura, y con la zona de subducción horizontal Pampeana. *19th Congreso Geológico Argentino*, Córdoba, 2 p.
- [24] Pilger, R.H. (1984) Cenozoic Plate Kinematics, Subduction, and Magmatism South American Andes. *Journal Geological Society of London*, **41**, 793-802.
<https://doi.org/10.1144/gsjgs.141.5.0793>
- [25] Marrett, R.A., Allmendinger, R.W., Alonso, R.N. and Drake, R.E. (1994) Late Ce-

- nozoic Tectonic Evolution of the Puna Plateau and Adjacent Foreland, Northwestern Argentine Andes. *Journal of South American Earth Sciences*, **7**, 179-207. [https://doi.org/10.1016/0895-9811\(94\)90007-8](https://doi.org/10.1016/0895-9811(94)90007-8)
- [26] Jordan, T.E., Schlunegger, F. and Cardozo, N. (2001) Unsteady and Spatially Variable Evolution of the Neogene Andean Bermejo Foreland Basin, Argentina. *Journal of South American Earth Sciences*, **14**, 775-798. [https://doi.org/10.1016/S0895-9811\(01\)00072-4](https://doi.org/10.1016/S0895-9811(01)00072-4)
- [27] Ramos, V.A., Cristallini, E.O. and Pérez, D.J. (2002) The Pampean Flat-Slab of the Central Andes. *Journal of South American Earth Sciences*, **15**, 59-78. [https://doi.org/10.1016/S0895-9811\(02\)00006-8](https://doi.org/10.1016/S0895-9811(02)00006-8)
- [28] Somoza, R. and Tomlinson, A. (2002) Los Andes Centrales del Sur durante el Neógeno: Observaciones e hipótesis sobre la cinemática horizontal. *15th Congreso Geológico Argentino*, El Calafate, 6 p.
- [29] Gutiérrez, A.A., Kojima, S. and Espinoza, R.S. (2002) Ambiente tectónico del distrito minero Agua de Dionisio (YMAD), Argentina. *11th Congreso Geológico Peruano*, Lima, 6 p.
- [30] Gutiérrez, A.A. and Mon, R. (2017) La faja plegada de antepaís del norte de Argentina. *20th Congreso Geológico Argentino*, Tucumán, 124-131.
- [31] Voll, G. (1961) New Work on Petrofabrics. *Geological Journal*, **2**, 503-567. <https://doi.org/10.1002/gj.3350020311>
- [32] Passchier, C.W. and Trouw, R.A.J. (2005) *Microtectonics*. 2nd Edition, Springer, Berlin, 366 p.
- [33] Schilling, F.R., Trumbull, R., Brasse, H., Haberland, C., Asch, G., Bruhn, D., Mai, K., Haak, V., Giese, P., Muñoz, M., Kummerow (Ramelow), J., Rietbrock, A., Ricaldi, E. and Vietor, T. (2006) Partial Melting in the Central Andean Crust: A Review of Geophysical, Petrophysical, and Petrologic Evidence. In: Oncken, O., Chong, G., Franz, G., Giese, P., Götze, H.-J., Ramos, V.A., Strecker, M.R. and Wigger, P., Eds., *The Andes: Active Subduction Orogeny*, *Frontiers in Earth Sciences*, Springer, Berlin, 459-474. https://doi.org/10.1007/978-3-540-48684-8_22
- [34] Sawyer, E.W. (2008) *Atlas of Migmatites*. The Canadian Mineralogist Special Publication 9, NRC Research Press, Ottawa, 371 p.
- [35] Sawyer, E.W., Cesare, B. and Brown, M. (2011) When the Continental Crust Melts. *Elements*, **7**, 229-234. <https://doi.org/10.2113/gselements.7.4.229>
- [36] Rosenberg, C.L. and Handy, M.R. (2005) Experimental Deformation of Partially-Melted Granite Revisited: Implications for the Continental Crustal. *Journal of Metamorphic Geology*, **23**, 19-28. <https://doi.org/10.1111/j.1525-1314.2005.00555.x>
- [37] Holtzman, B.K., Kohlstedt, D.L., Zimmerman, M.E., Heidelbach, F., Hiraga, T. and Hustoft, J. (2003) Melt Segregation and Strain Partitioning: Implications for Seismic Anisotropy and Mantle Flow. *Science*, **301**, 1227-1230. <https://doi.org/10.1126/science.1087132>
- [38] Jordan, T.E. and Allmendinger, R.W. (1986) The Sierras Pampeanas of Argentina: A Modern Analog of Rocky Mountain Foreland Deformation. *American Journal of Science*, **286**, 737-764. <https://doi.org/10.2475/ajs.286.10.737>
- [39] Kley, J., Monaldi, C.R. and Salfity, J.A. (1999) Along-Strike Segmentation of the Andean Foreland: Causes and Consequences. *Tectonophysics*, **301**, 75-94. [https://doi.org/10.1016/S0040-1951\(98\)90223-2](https://doi.org/10.1016/S0040-1951(98)90223-2)
- [40] Isacks, B.L. (1988) Uplift of the Central Andean Plateau and Bending of the Bolivian Orocline. *Journal of Geophysical Research*, **93**, 3211-3231.

<https://doi.org/10.1029/JB093iB04p03211>

- [41] Barazangi, M. and Isacks, B.L. (1976) Spatial Distribution of Earthquakes and Subduction of the Nazca Plate beneath South America. *Geology*, **4**, 686-692. [https://doi.org/10.1130/0091-7613\(1976\)4<686:SDOEAS>2.0.CO;2](https://doi.org/10.1130/0091-7613(1976)4<686:SDOEAS>2.0.CO;2)
- [42] Pilger, R.H. (1981) Plate Reconstructions, Aseismic Ridges, and Low-Angle Subduction beneath the Andes. *Geological Society of America Bulletin*, **92**, 448-456. [https://doi.org/10.1130/0016-7606\(1981\)92<448:PRARAL>2.0.CO;2](https://doi.org/10.1130/0016-7606(1981)92<448:PRARAL>2.0.CO;2)
- [43] Allmendinger, R.W., Ramos, V.A., Jordan, T.E., Palma, M. and Isacks, B.L. (1983) Paleogeography and Andean Structural Geometry, Northwest Argentina. *Tectonics*, **2**, 1-16. <https://doi.org/10.1029/TC002i001p00001>
- [44] Rossello, E.A., Urreiztieta, M., Le Corre, C., Cobbold, P.R. and Gapais, D. (1996) La Elipticidad del bajo La Alumbreira y la caldera del Cerro galán (Catamarca, Argentina): Reflejo de la deformación Andina? *RAGA*, **51**, 193-200.
- [45] González Bonorino, F. (1947) Carta Geológico-Económica Capillitas-12d, provincia de Catamarca, escala 1:200.000. Ministerio de Economía, Dirección General de Minas y Geología, Buenos Aires. Publicación SIC N° 65.
- [46] Mirré, J.C. and Aceñolaza, F.G. (1972) El hallazgo de Oldhamia sp. (traza fósil) y su valor como evidencia de edad Cámbrica para el supuesto Precámbrico del borde occidental del Aconquija, provincia de Catamarca. *Ameghiniana*, **9**, 72-78.
- [47] González Bonorino, F. (1950a) Descripción geológica de la Hoja 13e Villa Alberdi (Tucumán-Catamarca). Dirección Nacional de Geología y Minería, Boletín N° 74, Buenos Aires.
- [48] Mc Bride, S., Caelles, J.C., Clark, A.H. and Farrar, E. (1975) Paleozoic Radiometric Age Provinces in the Andean Basement, Latitudes 25°-30° S: Earth Planet. *Science Letters*, **29**, 373-383. [https://doi.org/10.1016/0012-821X\(76\)90142-4](https://doi.org/10.1016/0012-821X(76)90142-4)
- [49] Durand, F. (1980) Geología de la sierra de la Ovejera, provincia de Catamarca. Tesis Doctoral, Facultad de Ciencias Naturales, Universidad Nacional de Tucumán, Inédito.
- [50] Aceñolaza, F.G., Toselli, A.J., Duran, F.R. and Díaz Taddei, R. (1982) Geología y estructura de la región norte de Andalgalá, provincia de Catamarca. *Acta Geológica Lilloana*, **161**, 121-139.
- [51] Rasuk, J.L. (2012) Geología de la Falla Atajo entre 27°19'26"-27°22'47" LS. Seminario inédito. Facultad de Ciencias Naturales e IML de la Universidad Nacional de Tucumán, 50 p.
- [52] Llambías, E.J. (1970) Geología de los Yacimientos Mineros de Agua de Dionisio: Revista de la Asociación Argentina de Mineralogía. *Petrología y Sedimentología*, **2**, 2-32.
- [53] Llambías, E.J. (1972) Estructura del Grupo Volcánico Farallón Negro. Catamarca, República Argentina. *Revista de la Asociación Geológica Argentina*, **27**, 161-169.
- [54] Sasso, A.M. (1997) Geological Evolution and Metallogenetic Relationships of the Farallón Negro Volcanic Complex, NW Argentina. Thesis Doctoral, v. 1 y 2, Queen's University, Kingston.
- [55] Sasso, A.M. and Clark, A.H. (1999) The Farallón Negro Group, Northwest Argentina: Magmatic, Hydrothermal and Tectonic Evolution, and Implications for Cu-Au Metallogeny in the Andean Back-Arc. *SEG Discovery*, **34**, 1-18. <https://doi.org/10.5382/SEGnews.1998-34.fea>
- [56] Bossi, G.E. and Muruaga, C.M. (2009) Estratigrafía e inversión tectónica del "rift" neógeno en el Campo del Arenal, Catamarca, NO Argentina. *Andean Geology*, **36**,

- 311-341. <https://doi.org/10.4067/S0718-71062009000200007>
- [57] Turner, J.C. (1962) Estratigrafía de la region al naciente de Laguna Blanca (Catamarca). *Revista de la Asociación Geológica Argentina*, **17**, 11-46.
- [58] Galli, C.I., Caffè, P.J., Arnosio, M., Seggiaro, R. and Becchio, R. (2012) Análisis paleoambiental y procedencia de los depósitos Cenozoicos en el extremo suroeste de la Sierra de Aconquija, provincia de Catamarca. *Revista de la Asociación Geológica Argentina*, **69**, 596-610.
- [59] Ruskin, B.G., Dávila, F.M., Hoke, G.D., Jordan, T.E., Astini, R.A. and Alonso, R. (2011) Stable Isotope Composition of Middle Miocene Carbonates of the Frontal Cordillera and Sierras Pampeanas: Did the Paranaense Seaway Flood Western and Central Argentina? *Paleogeography, Palaeoclimatology, Palaeoecology*, **308**, 293-303. <https://doi.org/10.1016/j.palaeo.2011.05.033>
- [60] Herazo, D.L., Gutiérrez, A.A., Norriella, H. and Mon, R. (2017) Análisis morfoclimático y tectónico de abanicos aluviales antiguos en la zona centro de la provincia de Catamarca, Argentina. *20th Congreso Geológico Argentino*, Tucumán, 132-137.
- [61] Penck, W. (1920) Der Südrand der Puna de Atacama (NW Argentinien). Ab Handlungen Mathematisch-Physikalische Klasse der Sächsischen Akademie der Wissenschaften, Leipzig, Vol. 37, 1-420.
- [62] González Bonorino, F. (1972) Descripción Geológica de la Hoja 13c, Fiambalá, Provincia de Catamarca. Carta Geológico-Económica de la República Argentina. Boletín Dirección Nacional de Geología y Minería, No. 127, 1-75.
- [63] Sosis, M. (1972) Descripción Geológica de la Hoja 14d, Tinogasta, Provincias de Catamarca y La Rioja. Boletín Dirección Nacional de Geología y Minería, No. 129, 1-56.
- [64] Bossi, G.E., Georgieff, S.M., Muruaga, C.M., Ibáñez, L.M. and Sanagua, J.G. (2009) Los conglomerados sintectónicos de la Formación Las Cumbres (Plio-Pleistoceno), Sierras Pampeanas de La Rioja y Catamarca, Argentina. *Andean Geology*, **36**, 172-196. <https://doi.org/10.4067/S0718-71062009000200002>
- [65] Bossi, G.E., Villanueva García, A. and Sosa Gómez, J. (1989) Revisión de la magnetoestratigrafía del Neógeno del bolsón de Fiambalá (Prov. de Catamarca, Argentina). In Reunión sobre Geotranssectas de América del Sur, Transecta No. 6, Actas, Mar del Plata, 146-150.
- [66] Sosa Gómez, J., Bossi, G.E. and Villanueva García, A. (1993) Tectónica del Neógeno en el Bolsón de Fiambalá, Provincia de Catamarca. *Zentralblatt Geologie und Paläontologie*, **1**, 319-331.
- [67] Toselli, A., Durand, F., Rossi de Toselli, J., Cisterna, C.E., López, J.P., Sardi, F., Saavedra, J., Córdoba, G., Miró, R., Bossi, G.E., Sesma, P., Guido, E., Puchulu, M.E. and Ávila, J.C. (2018) Hoja Geológica 2966-I, Aimogasta, 1:250.000. Provincias de La Rioja y Catamarca. Servicio Geológico Minero Argentino, Boletín N° 433, 82 p.
- [68] Strecker, M.R. (1987) Nuevos datos neotectónicos sobre las sierras Pampeanas Septentrionales (26° -27° S), República Argentina. *10th Congreso Geológico Argentino*, S. M. de Tucumán, Actas I, 231-234.
- [69] Bossi, G.E., Georgieff, S.M., Gavrilloff, I., Ibáñez, L.M. and Muruaga, C.M. (2001) Cenozoic Evolution of the Intermontane Santa María Basin, Pampean Ranges, Northwestern Argentina. *Journal of South American Earth Science*, **14**, 725-734. [https://doi.org/10.1016/S0895-9811\(01\)00058-X](https://doi.org/10.1016/S0895-9811(01)00058-X)
- [70] Seggiaro, R., Caffè, P.J., Becchio, R., Galli, C., Arnosio, M. and Da Poián, G. (2014) Evolución tectónica Andina entre las sierras de Hualfin, Capillitas y extremo sur de

- Aconquija, provincia de Catamarca. *Revista de la Asociación Geológica Argentina*, **71**, 500-512.
- [71] Riller, U. and Oncken, O. (2003) Growth of the Central Andean Plateau by Tectonic Segmentation Is Controlled by the Gradient in Crustal Shortening. *Journal of Geology*, **111**, 367-384. <https://doi.org/10.1086/373974>
- [72] Cladouhos, T.T., Allmendinger, R.W., Coira, B. and Farrar, E. (1994) Late Cenozoic Deformation in the Central Andes: Fault Kinematics from the Northern Puna, Northwestern Argentina, and Southwestern Bolivia. *Journal of South American Earth Sciences*, **7**, 209-228. [https://doi.org/10.1016/0895-9811\(94\)90008-6](https://doi.org/10.1016/0895-9811(94)90008-6)
- [73] Marrett, R.A. and Strecker, M.R. (2000) Response of Intracontinental Deformation in the Central Andes to the Late Cenozoic Reorganization of South American Plate Motion. *Tectonics*, **19**, 452-467. <https://doi.org/10.1029/1999TC001102>
- [74] Allmendinger, R.W., Strecker, M.R., Eremchuk, J.E. and Francis, P. (1989) Neotectonic Deformation of the Southern Puna Plateau, Northwestern Argentina: *Journal of South American Earth Sciences*, **2**, 111-130. [https://doi.org/10.1016/0895-9811\(89\)90040-0](https://doi.org/10.1016/0895-9811(89)90040-0)
- [75] Mon, R. (2001) Estructuras curvadas y levantamientos verticales en la Cordillera Oriental (provincias de Salta y Tucumán). *Revista de la Asociación Geológica Argentina*, **56**, 367-376.
- [76] Vergani, G. and Starck, D. (1989) Aspectos estructurales del valle de Lerma, al sur de la ciudad de Salta. *Boletín de Informaciones Petroleras*, 4-9.
- [77] Comínguez, A.H. and Ramos, V.A. (1991) La estructura profunda entre Precordillera y Sierras Pampeanas de Argentina: Evidencias de la sísmica de reflexión profunda. *Revista Geológica de Chile*, **18**, 3-14.
- [78] Grier, M.E., Salfity, J.A. and Allmendinger, R.W. (1991) Andean Reactivation of the Cretaceous Salta Rift, Northwestern Argentina. *Journal of South American Earth Sciences*, **4**, 351-372. [https://doi.org/10.1016/0895-9811\(91\)90007-8](https://doi.org/10.1016/0895-9811(91)90007-8)
- [79] Zapata, T.R. and Allmendinger, R.W. (1996) La estructura de la Precordillera Oriental y valle de Bermejo a los 30° de latitud sur. 13° *Congreso Geológico Argentino*, Vol. 2, 211-224.
- [80] Mon, R. and Drozdowski, G. (1999) Cinturones doble vergentes en los Andes del norte argentino. Hipótesis sobre su origen. *Revista de la Asociación Geológica Argentina*, **54**, 3-8.
- [81] Jordan, T.E. and Alonso, R.N. (1987) Cenozoic Stratigraphy and Basin Tectonics of the Andes Mountains, 20°-28° South Latitude. *American Association of Petroleum Geologists Bulletin*, **71**, 49-64. <https://doi.org/10.1306/94886D44-1704-11D7-8645000102C1865D>
- [82] Strecker, M.R., Cervený, P., Bloom, A.L. and Malizia, D. (1989) Late Cenozoic Tectonism and Landscape Development in the Foreland of the Andes: Northern Sierras Pampeanas (26°-28°S), Argentina. *Tectonics*, **8**, 517-534. <https://doi.org/10.1029/TC008i003p00517>
- [83] Kleinert, K. and Strecker, M.R. (2001) Climate Change in Response to Orographic Barrier Uplift: Paleosol and Stable Isotope Evidence from the Late Neogene Santa María Basin, Northwestern Argentina. *Geological Society of America, Bulletin*, **113**, 728-742. [https://doi.org/10.1130/0016-7606\(2001\)113<0728:CCIRTO>2.0.CO;2](https://doi.org/10.1130/0016-7606(2001)113<0728:CCIRTO>2.0.CO;2)
- [84] Carrera, N. and Muñoz, J.A. (2008) Thrusting Evolution in the Southern Cordillera Oriental (Northern Argentine Andes): Constraints from Growth Strata. *Tectonophysics*, **459**, 107-122. <https://doi.org/10.1016/j.tecto.2007.11.068>
- [85] Gutiérrez, A.A., Mon, R., Arnous, A. and Aranda-Viana, R.G. (2021) Piedmont

- Deposits as Seismic Energy Dissipators, Sierras Pampeanas of Argentina. *Springer Nature Applied Sciences*, **3**, Article No. 887. <https://doi.org/10.1007/s42452-021-04874-0>
- [86] Löbens, S., Sobel, E.R., Bense, F.A., Wemmer, K., Dunkl, I. and Siegesmund, S. (2013) Refined Exhumation History of the Northern Sierras Pampeanas, Argentina. *Tectonics*, **32**, 453-472. <https://doi.org/10.1002/tect.20038>
- [87] Mortimer, E., Carrapa, B., Coutand, I., Schoenbohm, L., Sobel, E.R., Sosa Gomez, J. and Strecker, M.R. (2009) Fragmentation of a Foreland Basin in Response to Out-of-Sequence Basement Uplifts and Structural Reactivation: El Cajón-Campo del Arenal Basin, NW Argentina. *Geological Society of America Bulletin*, **119**, 637-653. <https://doi.org/10.1130/B25884.1>
- [88] Allmendinger, R.W. and Gubbels, T. (1996) Pure and Simple Shear Plateau Uplift: Altiplano-Puna, Argentina, and Bolivia. *Tectonophysics*, **259**, 1-13. [https://doi.org/10.1016/0040-1951\(96\)00024-8](https://doi.org/10.1016/0040-1951(96)00024-8)
- [89] Somoza, R. and Ghidella, M.E. (2005) Convergencia en el margen occidental de América del Sur durante el Cenozoico. 16° *Congreso Geológico Argentino, Actas*, La Plata, 43-45.
- [90] Lavenu, A. (2006) Neotectónica de los Andes entre 1° N y 47° S (Ecuador, Bolivia y Chile): Una revisión. *Revista de la Asociación Geológica, Argentina*, **61**, 504-524.
- [91] Proffett, J.M. (2003) Geology of the Bajo de la Alumbrera Porphyry Copper-Gold Deposit, Argentina. *Economic Geology*, **98**, 1535-1574. <https://doi.org/10.2113/gsecongeo.98.8.1535>
- [92] Palacio, M.B., Chernicoff, C.J. and Godeas, M.C. (2005) La estructura caldérica Vis-Vis asociada al volcanismo mioceno del distrito minero Farallón Negro, provincia de Catamarca. *Revista de la Asociación Geológica Argentina*, **60**, 609-612.
- [93] ASTER (Advanced Spaceborne Thermal Emission and Reflection Radiometer). <http://asterweb.jpl.nasa.gov>
- [94] ESA (European Space Agency). <https://sentinel.esa.int/web/sentinel/home>
- [95] USGS. <https://earthexplorer.usgs.gov>
- [96] Allmendinger, R.W., Cardozo, N. and Fisher, D. (2012) Structural Geology Algorithms: Vectors and Tensors in Structural Geology. Cambridge University Press, Cambridge. <https://doi.org/10.1017/CBO9780511920202>
- [97] Cardozo, N. and Allmendinger, R.W. (2013) Spherical Projections with OSXSte-reonet. *Computers & Geosciences*, **51**, 193-205. <https://doi.org/10.1016/j.cageo.2012.07.021>
- [98] Cross, T. and Pilger, R.H. (1982) Controls of Subduction Geometry, Location of Magmatic Arc, and Tectonics of Arc and Back-Arc Regions. *Geological Society of America Bulletin*, **93**, 545-562. [https://doi.org/10.1130/0016-7606\(1982\)93<545:CO&GLO>2.0.CO;2](https://doi.org/10.1130/0016-7606(1982)93<545:CO&GLO>2.0.CO;2)
- [99] Gutiérrez, A.A., Mon, R. and Suvires, G.M. (2017c) La red de drenaje del borde oriental Andino y de la llanura central Argentina, indicadora de movimientos tectónicos recientes. *Ciencias de la Tierra y Recursos Naturales del NOA, Relatorio del XX Congreso Geológico Argentino*, Tucumán, 646-669.
- [100] Bossi, G.E. and Palma, R. (1982) Reconsideración de la estratigrafía del valle de Santa María, provincia de Catamarca, Argentina. 5° *Congreso Latinoamericano de Geología, Actas*, Buenos Aires, Vol. 1, 155-172.
- [101] Sylvester, A.G. (1988) Strike-Slip Faults. *Geological Society of American Bulletin*, **100**, 1666-1703. [https://doi.org/10.1130/0016-7606\(1988\)100<1666:SSF>2.3.CO;2](https://doi.org/10.1130/0016-7606(1988)100<1666:SSF>2.3.CO;2)

- [102] Bull, W.B. (2007) *Tectonic Geomorphology of Mountains: A New Approach to Paleoseismology*. Blackwell Publishing, Hoboken, 316 p.
<https://doi.org/10.1002/9780470692318>
- [103] Rodgers, D. and Rizer, W.D. (1981) Deformation and Secondary Faulting near the Leading Edge of a Thrust Fault. *Geological Society, London, Special Publications*, **9**, 65-77. <https://doi.org/10.1144/GSL.SP.1981.009.01.07>
- [104] Ikeda, Y. (1983) Thrust Front Migration and Its Mechanisms-Evolution of Intraplate Thrust Fault Systems. *Bulletin of the Geography Department, University of Tokyo*, **15**, 125-159.
- [105] Mon, R., Monaldi, C.R. and Salfity, J.A. (2005) Curved Structures and Interference Fold Patterns Associated with Lateral Ramps in the Eastern Cordillera, Central Andes of Argentina. *Tectonophysics*, **399**, 173-179.
<https://doi.org/10.1016/j.tecto.2004.12.021>
- [106] Gapais, D., Urreiztieta, M., Le Corre, C., Rosello, E.A. and Cobbold, P.R. (1992) Cenozoic Tectonics and Basin Development at the Southern Border of the Altiplano-Puna, NW Argentina: A Preliminary Analysis. *International Symposium on "Geodynamic Evolution of Sedimentary Basins"*, Moscú, 1 p.
- [107] Nalpas, T., Townley, B. and Sanhueza, D. (2011) Influencia de un bloque rígido en un sistema de fallas de rumbo: modelamiento análogo. *Andean Geology*, **38**, 23-36.
<https://doi.org/10.5027/andgeoV38n1-a03>
- [108] Gutiérrez, A.A., Mon, R. and Cisterna, C.E. (2018) Nivel de exposición de yacimientos minerales, YMAD caso de estudio. Editorial Académica Española, Madrid, 53 p.